

UNIVERSITY OF OKLAHOMA

GRADUATE COLLEGE

VALIDATION OF PORTABLE HANDHELD X-RAY
FLUORESCENCE (PHXRF) ON STABILIZED SUBGRADE PROJECTS
FOR CONSTRUCTION QUALITY CONTROL AND GEOTECHNICAL
FORENSIC INVESTIGATIONS

A THESIS

SUBMITTED TO THE GRADUATE FACULTY

in partial fulfillment of the requirements for the

Degree of

MASTER OF SCIENCE

By

NATHAN FERRARO
Norman, Oklahoma
2016

VALIDATION OF PORTABLE HANDHELD X-RAY
FLUORESCENCE (PHXRF) ON STABILIZED SUBGRADE PROJECTS
FOR CONSTRUCTION QUALITY CONTROL AND GEOTECHNICAL
FORENSIC INVESTIGATIONS

A THESIS APPROVED FOR THE
SCHOOL OF CIVIL ENGINEERING AND ENVIRONMENTAL SCIENCE

BY

Dr. Amy Cerato, Chair

Dr. Gerald Miller

Dr. Kanthasamy Muraleetharan

© Copyright by NATHAN FERRARO 2016
All Rights Reserved.

To friends and family for their unwavering support throughout the years
and to the many mentors who showed me that my biggest obstacle was self-doubt,
I dedicate this thesis.

ACKNOWLEDGEMENTS

I would like to offer his sincerest gratitude to Dr. Amy B. Cerato, Rapp Foundation Presidential Professor at the University of Oklahoma's School of Civil Engineering and Environmental Science (CEES), for her invaluable guidance throughout the course of my graduate studies. Her mentorship and persistent encouragement have allowed me to achieve more academically and professionally than I thought was possible. For these reasons, amongst many others, I am extraordinarily grateful and feel truly blessed.

Many thanks are extended to Dr. Robert Nairn, Sam K. Viersen Family Foundation Presidential Professor of CEES, and Rick Ramsey, Senior Sales Representative of Houston Analytical Systems Co., for generously allowing me to borrow their XRF spectrometers for this research. Similar gratitude is extended to the staff of the Materials Division at the Oklahoma Department of Transportation for opening up their laboratory to me and assisting me with soil sample preparation. The benevolence of these individuals significantly improved the efficiency of the experiments, saving both time and money, for which I am extremely appreciative.

To Dr. Gerald Miller, Rodney Collins, and Dr. Wassim Tabet, thank you for all of your assistance with this project. The reduction in workload for me in the field aspects was very much appreciated. Additionally, your advice during the analysis and writing of this thesis was invaluable.

Furthermore, I would like to thank the Southern Plains Transportation Center (SPTC) for providing financial support throughout the entirety of this research. Plainly, this research would not be possible without your continued support.

Last, but certainly not least, I would like to thank my family and friends. My family's backing has allowed me to fully focus on my studies and serve the world of academia at a higher level. My friends' fellowship has greatly enriched my education and, at times, has helped me maintain my sanity. Simply put, I would not have completed this thesis without the help from both. Thank you so much.

TABLE OF CONTENTS

Acknowledgements	iv
List of Figures.....	ix
List of Tables	xiii
Abstract.....	xv
Chapter 1: Introduction.....	1
1.1 Introduction	1
1.2 Purpose and Goals	5
1.3 Scope	6
Chapter 2: Literature Review	7
2.1 Introduction	7
2.2 Current Subgrade Stabilization Construction Methods	7
2.2.1 Subgrade Preparation.....	9
2.2.2 Subgrade Pulverization and Scarification	9
2.2.2.1 Pulverization Requirements for Cement Treated Subgrades.....	10
2.2.2.2 Pulverization Requirements for Lime Treated Subgrades.....	11
2.2.3 Application of Stabilizing Agent.....	12
2.2.3.1 Application Requirements for Cement Treated Subgrades	12
2.2.3.2 Application Requirements for Lime Treated Subgrades	13
2.2.4 Mixing	14
2.2.4.1 Mixing Requirements for Cement Treated Subgrades	14
2.2.4.2 Mixing Requirements for Lime Treated Subgrades	15
2.2.5 Compaction.....	16

2.3 XRF Spectrometry	17
Chapter 3: Methods	23
3.1 Materials and Apparatuses	23
3.2 Testing Matrix	24
3.2.1 Laboratory Testing	24
3.2.2 Field Testing.....	25
3.3 Mixing Procedures.....	26
3.4 Milling Procedures	29
3.5 Pressed Pellet Procedures	30
3.6 Powder Samples Procedures.....	31
3.7 Laboratory Testing of PHXRF	33
3.8 Laboratory Testing Data Analysis.....	35
3.9 Field Testing of PHXRF.....	36
3.10 Field Testing Data Analysis	40
Chapter 4: Results.....	41
4.1 Introduction	41
4.2 PHXRF Laboratory Testing	41
4.2.1 Scan Durations.....	41
4.2.2 Scan Technique	47
4.2.3 Particle Size.....	53
4.2.4 Sample Type.....	62
4.2.5 PHXRF Device Comparison	69
4.3 PHXRF Field Testing.....	71

4.3.1 In Situ PHXRF Measurement Accuracy	71
4.3.2 Ex Situ PHXRF Measurement Accuracy	74
4.3.3 Spatial Stabilizer Heterogeneity	76
4.3.3.1 Site 1	76
4.3.3.2 Site 2	79
4.3.3.3 Site 3	80
4.3.4 Depth Stabilizer Heterogeneity	83
4.3.4.1 Site 1	84
4.3.4.2 Site 2	85
4.3.4.3 Site 3	86
Chapter 5: Conclusions and Recommendations	88
5.1 Conclusions	88
5.2 Recommendations for Future Research.....	93
Chapter 6: Schedule.....	94
Chapter 7: References.....	95

LIST OF FIGURES

Figure 1: Example of Scarifying the Subgrade	10
Figure 2: Self-Powered Mechanical Rotor Mixers.....	15
Figure 3: XRF Emitted from a Radiated Bromine Atom (Bruker 2013)	19
Figure 4: Effect of Particle Size on Length of XRF Path.....	21
Figure 5: Mixing Samples with a Mechanical Blender	28
Figure 6: SPEX Shatterbox 8515 Used to Mill Samples.....	30
Figure 7: Removing Plunger from SPEX Evacuable Die Set	31
Figure 8: XRF Powder Sample.....	32
Figure 9: Poorly Prepared Powder Sample (Left) and	33
Figure 10: (Left) Bruker S1 Titan in Desktop Stand and (Right) Thermo Scientific Niton XL3t GOLDD+ in Field Stand.....	34
Figure 11: Dividing Powder Samples into Four Quadrants	35
Figure 12: Locations of Field Test Sites 1, 2, and 3.....	37
Figure 13: Spatial XRF Testing and Sampling Locations in the Field.....	38
Figure 14: Hammer Head Soil Probe Used to Retrieve Samples at Various Depths	40
Figure 15: Effects of Various Scan Durations on Precision and Accuracy of S1 Titan PHXRF Device for (a) 60 Second (30 - 30), (b) 60 Second (15 - 45), (c) 75 Second (15 -60), and (d) 135 Second (15 - 120) Scan Durations on OHC samples.	45
Figure 16: Effects of Various Scan Durations on Precision and Accuracy of S1 Titan PHXRF Device for (a) 60 Second (30 - 30), (b) 60 Second (15 - 45), (c) 75 Second (15 - 60), and (d) 135 Second (15 - 120) Scan Durations on SGB samples.....	46

Figure 17: Beam Footprints of the S1 Titan (Left) and Niton XL3t (Right) PHXRF Devices	49
Figure 18: Effects of (a) Standard and (b) Quartering Scan Techniques on Precision and Accuracy of S1 Titan PHXRF Device for OHC Samples.....	51
Figure 19: Effects of (a) Standard and (b) Quartering Scan Techniques on Precision and Accuracy of Niton XL3t PHXRF Device for OHC Samples.	51
Figure 20: Effects of (a) Standard and (b) Quartering Scan Techniques on Precision and Accuracy of S1 Titan PHXRF Device for SGB Samples.....	52
Figure 21: Effects of (a) Standard and (b) Quartering Scan Techniques on Precision and Accuracy of Niton XL3t PHXRF Device for SGB Samples.....	52
Figure 22: Effects of Various Particle Sizes on Precision and Accuracy of S1 Titan PHXRF Device for (a) Passing No. 4, (b) Passing No. 40, (c) Passing No. 100, and (d) Passing No. 200 particle size OHC samples.....	57
Figure 23: Effects of Various Particle Sizes on Precision and Accuracy of Niton XL3t PHXRF Device for (a) Passing No. 4, (b) Passing No. 40, (c) Passing No. 100, and (d) Passing No. 200 particle size OHC samples.....	58
Figure 24: Effects of Various Particle Sizes on Precision and Accuracy of S1 Titan PHXRF Device for (a) Passing No. 4, (b) Passing No. 40, (c) Passing No. 100, and (d) Passing No. 200 particle size SGB samples.	59
Figure 25: Effects of Various Particle Sizes on Precision and Accuracy of Niton XL3t PHXRF Device for (a) Passing No. 4, (b) Passing No. 40, (c) Passing No. 100, and (d) Passing No. 200 particle size SGB samples.	60
Figure 26: Average RMSD and Average COV_{RMSD} as a Function of Particle Size.....	62

Figure 27: Effects of (a) Pressed Pellet and (b) Powder Sample Types on Precision and Accuracy of S1 Titan PHXRF Device for OHC Samples.....	66
Figure 28: Effects of (a) Pressed Pellet and (b) Powder Sample Types on Precision and Accuracy of Niton XL3t PHXRF Device for OHC Samples.....	66
Figure 29: Effects of (a) Pressed Pellet and (b) Powder Sample Types on Precision and Accuracy of S1 Titan PHXRF Device for SGB Samples.....	67
Figure 30: Effects of (a) Pressed Pellet and (b) Powder Sample Types on Precision and Accuracy of Niton XL3t PHXRF Device for SGB Samples.....	67
Figure 31: RMSD for OHC (Left) and SGB (Right) Pellet and Powder Samples.....	68
Figure 32: Direct Comparison of S1 Titan and Niton XL3t Measurements for OHC Samples (Left) and SGB Samples (Right).....	71
Figure 33: Linear Regression of Site 2 In Situ Measurements with the Niton XL3t PHXRF.....	73
Figure 34: Linear Regression of Site 2 Ex Situ Measurements with the Niton XL3t PHXRF.....	76
Figure 35: Idealized and Corrected Spatial Stabilizer Distribution for Site 1 at Depths of (a) 0 - 3, (b) 3 - 6, (c) 6 - 9, and (d) 9 - 12 Inches	78
Figure 36: Idealized and Corrected Spatial Stabilizer Distribution for Site 2 at Depths of (a) 0 - 3, (b) 3 - 6, (c) 6 - 9, and (d) 9 - 12 Inches	80
Figure 37: Idealized and Corrected Spatial Stabilizer Distribution for Site 3 at Depths of (a) 0 - 3, (b) 3 - 6, (c) 6 - 9, and (d) 9 - 12 Inches	82
Figure 38: Depth Heterogeneity for All Sites.....	84
Figure 39: Idealized (Left) and Corrected (Right) Depth Heterogeneity for Site 1	85

Figure 40: Idealized (Left) and Corrected (Right) Depth Heterogeneity for Site 2 86

Figure 41: Idealized (Left) and Corrected (Right) Depth Heterogeneity for Site 3 87

LIST OF TABLES

Table 1: Differences in Stabilization Specifications for Pulverization of Subgrade Soils in Preparation for Cement Treatment	11
Table 2: Differences in Stabilization Specifications for Pulverization of Subgrade Soils in Preparation for Lime Treatment	12
Table 3: Differences in Stabilization Specifications for Compaction of Subgrade Soils	17
Table 4: Testing Matrix Showing Number of Scans (S1 Titan / Niton XL3t) of all Seventy Unique Samples and their Corresponding Soil Types, Stabilizer Contents, Sample Types, and Maximum Particle Sizes	25
Table 5: Proportions of Soil and Stabilizer to Achieve a Range of Stabilizer Contents	27
Table 6: Effects of Scan Duration on STDEV, COV _{STDEV} , RMSD, and COV _{RMSD} for OHC Samples	43
Table 7: Effects of Scan Duration on STDEV, COV _{STDEV} , RMSD, and COV _{RMSD} for SGB Samples	43
Table 8: Effects of Scan Technique on STDEV, COV _{STDEV} , RMSD, and COV _{RMSD} for OHC Samples	47
Table 9: Effects of Scan Technique on STDEV, COV _{STDEV} , RMSD, and COV _{RMSD} for SGB Samples	48
Table 10: Effects of Particle Size on STDEV, COV _{STDEV} , RMSD, and COV _{RMSD} for OHC Samples	54
Table 11: Effects of Particle Size on STDEV, COV _{STDEV} , RMSD, and COV _{RMSD} for SGB Samples	55

Table 12: Average RMSD and COV_{RMSD} for All Samples and Both PHXRF Devices.	61
Table 13: Effects of Sample Type on $STDEV$, COV_{STDEV} , RMSD, and COV_{RMSD} for OHC Samples	63
Table 14: Effects of Sample Type on $STDEV$, COV_{STDEV} , RMSD, and COV_{RMSD} for SGB Samples.....	64
Table 15: Direct Comparison of S1 Titan and Niton XL3t Measurements.....	70
Table 16: Precision and Accuracy of Niton XL3t In Situ	72
Table 17: Precision and Accuracy of Niton XL3t Ex Situ	75
Table 18: Average Measured Stabilizer Contents and Design Stabilizer Contents for Top Nine Inches of All Sites	83

ABSTRACT

Problematic subgrade soils are often strengthened using various amounts of chemical stabilizers, such as lime, cement kiln dust, and fly ash. The soil becomes strengthened and more resistant to volume changes through pozzolanic reactions, cementing, or a combination of the two. The amount of stabilizer needed for a particular soil to increase its strength to a minimum value is not codified and typically requires a lengthy mix-design. In addition, once this amount of stabilizer is determined, placed, mixed, and compacted in the field, there is no good way to determine how much stabilizer ends up in the design depth of subgrade. Current quality control methods are too laborious or inaccurate. Furthermore, there is no sophisticated way of assessing stabilization homogeneity throughout the site area and design depth. All of these shortcomings cause problems not only from a construction quality control standpoint, but from a geotechnical forensic investigation standpoint as well.

Faulty subgrades are one of the most costly issues to correct; while ironically, their construction is often the least expensive part of a roadway job. If the subgrade does not provide adequate strength and stiffness for the pavement system above, then poor roadway performance is eminent and, in many cases, the roadway will need to be removed to access the subgrade for remediation. In order to better control the quality of subgrade stabilization and mitigate these costly repairs, an old technology with a new purpose has been developed. X-ray Fluorescence (XRF) has been found to accurately measure the amount of calcium, which is the main element in many chemical stabilization products, in treated subgrade soils. This study focuses on extending the successes found using

commercial laboratory XRF spectrometry to portable handheld XRF (PHXRF) spectrometry.

PHXRF devices are heavily used for qualitative analysis in dozens of industries for a broad range of applications. Examples include environmental testing (e.g. detection of heavy metals such as lead, zinc, and mercury in soil), metal sorting (e.g. positive material identification), and pharmaceutical testing (e.g. drug impurities and vitamin extraction) amongst others. The latest literature trends towards expanding these PHXRF practices to quantitative measures, but is somewhat limited when it comes to lighter elements (i.e. calcium) and soil analysis. This research looks to help remedy this void in the literature by verifying the accuracies of two PHXRF spectrometers by comparing their stabilizer content (*SC*) measurements to measurements made by a proven commercial laboratory.

This research was divided into two major phases: laboratory testing and field testing. In the laboratory testing portion, engineered samples with known *SC* were created to evaluate the accuracy of the PHXRF devices and to identify the necessary amount of preparation needed to produce accurate results. Since sample preparation is known to have the greatest influence on the accuracy of the PHXRF spectrometers, a matrix of 70 samples of varying degrees of preparation was created. The independent variables that were examined in these samples are sample type (i.e. powder samples and pressed pellets), particle diameter (i.e. 4.76 mm, 0.420 mm, 0.149 mm, and 0.074 mm), and *SC* (i.e. 0 to 64%). A range of *SC*s were achieved by mixing calculated amounts of either hydrated lime, cement kiln dust, or fly ash with the soil. Over 2,200 total scans were

completed with two XRF spectrometers, a Bruker S1 Titan and a Thermo Scientific Niton XL3t.

In the field testing portion, three roadway construction sites that required subgrade stabilization were analyzed using the Niton XL3t. Spatial variability was investigated by taking measurements in a grid pattern. Distances between readings were five feet along both the length and width of the grid. Additionally, depth variability was investigated by taking 12 inch deep pre-treatment and post-treatment samples throughout the grid. These samples were separated into four depths (i.e. 0-3 in, 3-6 in, 6-9 in, and 9-12 in), prepared into powder samples, and analyzed with the PHXRF device. Random samples were sent to a verified commercial XRF laboratory for analysis, and then the *SC*s determined by the commercial laboratory were compared to those determined by the PHXRF device to assess device accuracy.

The results from the laboratory phase of the experiment are that longer scan durations do not increase precision or accuracy of PHXRF *SC* measurements, effects of different scanning techniques on the accuracy of PHXRF *SC* are inconclusive, samples with smaller particle sizes produce more accurate measurements, effects of sample type on the precision and accuracy of PHXRF *SC* measurements are inconclusive, and both PHXRF devices are adequate for determining *SC* in subgrade soils. The S1 Titan, however, performed better with OHC samples while the Niton XL3t performed better with SGB samples. The results from the field phase of the experiment are that in situ PHXRF *SC* measurements yield sporadic and inadequate readings, ex situ measurements are capable of producing representative measurements when corrected mathematically with a linear regression equation, spatial *SC* heterogeneity can be assessed with PHXRF

spectrometry, and depth *SC* heterogeneity can be assessed with PHXRF spectrometry. Ultimately, PHXRF spectrometry shows great promise in construction quality control and forensic geotechnical investigations; however, further development may be necessary before this technology is implemented.

CHAPTER 1

INTRODUCTION

1.1 Introduction

A sizable portion of roadway construction projects in the southern plains states (i.e. Arkansas, Louisiana, Oklahoma, New Mexico, and Texas) require subgrade stabilization to combat an assortment of problematic soil behavior. Some of these conditions include low strength subgrades, high swell potential soils, and/or high collapse potential soils, all of which are troublesome for the transportation industry across this region. In Oklahoma alone, nearly 46% of major roadways are considered to be in poor or mediocre working condition because of these subgrade weaknesses (Solanki, et al. 2009). Many of these issues are remedied by chemical subgrade stabilization, which is typically achieved by adding cementitious chemical agents and water to the soil. This method of subgrade improvement has been heavily studied and proven to be advantageous, both in terms of performance and cost.

Design and construction procedures for subgrade stabilization are somewhat standard throughout the southern plains region with minor variations between each state (Arkansas State Highway and Transportation Department 2014; New Mexico Department of Transportation 2014; Texas Department of Transportation 2014; Oklahoma Department of Transportation 2009; Louisiana Department of Transportation and Development 2006). Yet surprisingly, roadway design specifications lack procedures detailing quality control measures. Many of the subgrade specifications mention no quality control methods and others mention either a dye indicator test or a titration

method. The dye indicator test (i.e. Phenolphthalein Test) while convenient, only detects the presence of a stabilizing agent, not the amount (National Lime Association 2004). The titration method (ASTM D3155-11) is capable of producing quantitative measurements, but it is complex, requires the user to handle harsh chemicals, requires the user to mix upwards of six reference solutions, and has questionable accuracy due to a large operator bias (Cerato and Miller 2013; ASTM D3155-11). The limits of both the dye indicator and titration methods necessitate the development of a new, more accurate, and more repeatable quality control technique.

Quality control of stabilized subgrades is particularly important because unsatisfactory subgrades are extremely expensive to fix. Tim Gatz, the Deputy Director of the Oklahoma Department of Transportation (ODOT), summarized it best when he stated, “Subgrades are the cheapest part of roadway construction, but the most costly to repair,” (Gatz 2015). This is because mending faulty subgrades often requires the complete removal of the roadway. Thus, it is only logical to invest in improving our current subgrade stabilization quality control protocols in order to mitigate such repairs in the future.

A reasonable method to fill this void is X-ray fluorescence (XRF) spectrometry. XRF spectrometry is an analysis technique used to determine the elemental makeup of a material. XRF has been around for over 100 years and has been developed to the point where its application is now practical. New handheld devices make XRF spectrometry portable, which could potentially make it a convenient and powerful tool in the field. Industries, such as metal sorting, mining, and environmental analysis, have used portable handheld XRF (PHXRF) spectrometry for positive material identification and trace

element detection for years now with great success. The archaeology industry has also been transformed by PHXRF because of its non-destructive analysis measures, convenience, speed, and cost-effectiveness (Shackley 2011). This technology has been particularly useful and beneficial in all of these other industries, so this begs the question, “Why not geotechnical engineering?”

Despite the past successes of PHXRF spectrometry, this technology has yet to be used to determine chemical stabilizer content, *SC*, in subgrade soils. Soil analysis, in general, has been limited in the XRF industry due to its complex and variable nature. Nearly an unlimited amount of soil mineralogies can exist, which makes crafting a comprehensive soil calibration library a difficult task. With that being said, sophisticated soil calibrations are becoming more common in the XRF industry as demand increases (Ramsey 2014). The two PHXRF devices used in this research were equipped with factory installed soil calibrations, which allowed for the accurate detection of key elements in stabilized soil samples.

Since chemical stabilizers typically used in subgrade stabilization projects are calcium-based and XRF spectrometry is capable of detecting individual elements such as calcium, it is reasonable to believe that this technology can be used to determine *SC*. By simply measuring the amounts of calcium in the chemical stabilizer, raw or untreated subgrade soil, and treated subgrade soil, one can back calculate the percentage of chemical stabilizer present in the treated soil. Ultimately, PHXRF spectrometry can give on-site inspectors the ability to verify that the amount of stabilizer prescribed actually matches the amount of stabilizer present in the ground. This enables them to remediate deficient areas before any pavement is poured, possibly saving the transportation industry

substantial amounts of money in repair cost by producing consistent and higher quality subgrades the first time.

This approach aligns with the ODOT's vision of infrastructural preservation. Mike Patterson, the Executive Director of the ODOT, said in the 2015 SPTC conference in Oklahoma City that, "Initial costs [of stabilization] may seem daunting; however, it can save us dividends in the long run by reducing maintenance and repair costs. In other words, pay now or pay more later." The large cost of remediating a faulty subgrade far outweighs the cost of purchasing a PHXRF spectrometer and performing a more thorough inspection during subgrade preparation. Thus, it would be in the best financial interest of the transportation industry to explore this option.

Similarly, XRF spectrometry can have collateral benefits from a forensic perspective. The question faced by construction inspectors is the same faced by forensic investigators: Does the amount of chemical stabilizer in the soil match the amount prescribed by the design engineers? XRF spectrometry may be used retroactively to make these determinations on a failed subgrade because elemental content does not change over time. Samples can be taken from the stabilized subgrade, bagged, and stored for future laboratory testing or the roadway could be cored and determinations made on site, increasing the efficiency of the investigation by saving time. Based on these measurements, an investigator can quickly and accurately determine whether the subgrade was inadequately constructed or inadequately designed (or both) and assign liability accordingly.

This research was necessary to assess if PHXRF spectrometry is a viable option for construction quality control and forensic geotechnical investigations. This research

focused on the accuracy and practicality of implementing PHXRF in the field and determining if it could be a useful tool in improving the quality of stabilized subgrades. Ultimately, PHXRF be helpful in helping the transportation industry deliver safer and more reliable roadways to the nation's motorists.

1.2 Purpose and Goals

Roadways in the United States are vital lifelines for its citizens. Over the course of 2009, 210 million drivers traveled over 3 trillion miles on these paved arteries (United States Department of Transportation 2011). The total mileage driven per year has rapidly increased over the last few decades, and it is expected to continue increasing in the foreseeable future. Estimates place total mileage driven in 2020 at 3.2 trillion (United States Department of Transportation 2000). The heavy use of these roadways highlights the importance of sound construction by today's contractors and thorough design and quality control by today's civil engineers.

The need for improved quality control and forensic geotechnical investigative methods is necessary to improve the safety of our transportation infrastructure. As cited by the National Highway Traffic Safety Administration (NHTSA), there were 52,000 motor vehicle crashes, of the nearly 2.2 million investigated, caused by environment-related critical reasons (Singh 2015). If any of these 52,000 crashes can be prevented by higher quality roadway construction or by a lesson learned from a proper forensic investigation as a result of this research, then this work can be considered a success.

The purpose of this research is to validate PHXRF on stabilized subgrade projects for construction quality control and forensic geotechnical investigations. Upon

validation, PHXRF would replace current methods for determining *SC* in subgrade soils. Ultimately, the goal is to provide American motorists with safer and more dependable roads and highways by reducing construction error.

To achieve these goals, a series of questions must be answered. The main questions of this research are as follows:

1. What preparation technique yields the most accurate PHXRF *SC* measurements?
Is this preparation technique feasible in the field?
2. What PHXRF device and analysis method should be used to achieve the most accurate PHXRF *SC* measurements?
3. What is the precision and accuracy of in situ and ex situ PHXRF *SC* measurements? Is PHXRF a viable option for measuring *SC* in stabilized subgrade soils?
4. Is PHXRF a viable option for assessing spatial and depth homogeneity in the field?

1.3 Scope

This work is phase two and three of a three phase research project. The first phase was a feasibility study of whether or not a commercial XRF laboratory could determine *SC* in stabilize subgrade soils and was detailed in Cerato and Miller (2013). Phase two continues that initial work to determine if PHXRF devices are capable of producing comparable *SC* measurements to those of commercial laboratories. The third phase of this research project aims to validate the accuracy of the PHXRF devices in the field where conditions are more erratic and sample preparation is minimal.

CHAPTER 2

LITERATURE REVIEW

2.1 Introduction

Current subgrade stabilization construction methods as well as principles and applications of XRF spectrometry are discussed. Additionally, potential limitations of XRF spectrometry as it relates to determining *SC* in subgrade soils will be examined.

2.2 Current Subgrade Stabilization Construction Methods

Subgrade stabilization is often used to address an assortment of problematic soil behavior. Some of the well-known and well-studied issues are low strength, which has been known to cause subgrade and pavement deformation, potholes, and rutting (Elliot, et al. 1998; Huang 1993; Majidzadeh, et al. 1978), high swell potential, which often plagues lightweight pavements and causes upwards of 7 billion dollars' worth of auto damage each year in the United States (Mishra 2007; Fredlund 1987; Krohn and Slosson 1980), and high collapse potential, which causes tremendous amounts of damage to highway infrastructure and poses significant challenges to geotechnical engineers (Howayek 2011; Houston 2002; Lawton, et al. 1992; Houston 1988). These problems, amongst others, are usually mitigated by mixing calcium-based chemical stabilizing agents, typically lime (Athanasopoulou 2014; Bell 1989; Holland and Griffin 1980;), fly ash (Athanasopoulou 2014; Lin, et al. 2013; Li, et al. 2009; Aykut, et al. 2006; Arora and Aydilck 2005; Koliass, et al. 2005), cement kiln dust (CKD) (Salahudeen, et al. 2014;

Parsons, et al. 2004), or Portland cement (Kolias, et al. 2005; Holland and Griffin 1980) with the native soil or fill.

In order to appreciate why an improved quality control technique for stabilized subgrade projects is necessary, a thorough understanding of current construction methods is crucial. To do this, a survey of subgrade stabilization methods in the southern plains states was conducted. The states and their respective standards are as follows:

- Arkansas: Arkansas 2003 Standard Specification for Highway Construction Division 300 Section 301.04
- Louisiana: 2006 Standard Specifications for Roads and Bridges Manual Sections 303 and 304
- New Mexico: 2014 Standard Specifications for Highway and Bridge Construction Division 300 Section 306.3
- Oklahoma: 2009 Standard Specifications Book Chapter 300 Section 307.04
- Texas: 2004 Standard Specifications for Construction and Maintenance of Highways, Streets, and Bridges Item 260.4

The steps of stabilization within the specifications are subgrade preparation, pulverization and scarification, application of stabilizing agent, mixing, and compaction. These steps are covered in individual sub-sections within each specification. Many stabilization steps are similar between states, however, there are some notable differences which will be

discussed. Possible sources of error in terms of *SC* and stabilizer distribution will be identified after each step, if applicable.

2.2.1 Subgrade Preparation

This stabilization step discusses shaping the subgrade to the design crown and grading and compacting it to the design density, after which the area is proof rolled and any soft spots are corrected. Subgrade preparation procedures are the same in all of the southern plains roadway design specifications.

2.2.2 Subgrade Pulverization and Scarification

This section provides instructions on how to achieve a proper soil gradation and homogenize the subgrade material in terms of density and moisture content throughout its design depth, which is typically 8 inches. Additionally, it discusses how to loosen the subgrade soil throughout its design depth as well as remove any materials larger than the material diameter limitations. This section stresses that it is critical that the soil beneath the treated subgrade depth is left undisturbed so that its strength is not decreased. The process of scarification is the same throughout the region, while pulverization varies slightly from state to state for both cement and lime stabilization treatments. Scarification is illustrated in Figure 1.



Figure 1: Example of Scarifying the Subgrade

Pulverization and scarification of the subgrade are important steps in the stabilization process, particularly for lime stabilization. When properly completed, both allow for more thorough mixing of the subgrade material and stabilizing agent as well as permit better compaction of the soil skeleton (Army and Air Force 1994). Despite this, spatial heterogeneity still tends to be an issue due to the presence of agglomerated elemental concentrations throughout the site (Army and Air Force 1994). These bulk aggregates are problematic because they allow the stabilizing agent to only react with the shell of the aggregate, leaving the core untreated.

2.2.2.1 Pulverization Requirements for Cement Treated Subgrades

Differences observed in pulverization requirements for cement treated subgrades are presented in Table 1. Basically, this section of the design specifications discusses the allowable maximum particle size of

milled roadbed material to be stabilized and how much of the roadbed material must be smaller than the maximum size.

Table 1: Differences in Stabilization Specifications for Pulverization of Subgrade Soils in Preparation for Cement Treatment

<i>State</i>	<i>% Passing #4 Sieve</i>	<i>% Passing 2.5" Sieve</i>	<i>Additional Requirements</i>
<i>Arkansas</i>	<i>80</i>		<i>Discard material retained on 3" sieve</i>
<i>Louisiana</i>	<i>60</i>		<i>No maximum material size</i>
<i>New Mexico</i>	<i>80</i>		<i>Discard material retained on 3" sieve</i>
<i>Oklahoma</i>		<i>75</i>	<i>Reduce material retained on 3" sieve until passing</i>
<i>Texas</i>		<i>100</i>	

2.2.2.2 Pulverization Requirements for Lime Treated Subgrades

The differences in the requirement for pulverization for future lime treatment between various states is similar to that of cement treatment, as seen in Table 2. They encompasses the allowable maximum particle size of milled roadbed material to be stabilized and how much of the roadbed material must be smaller than the maximum size.

Table 2: Differences in Stabilization Specifications for Pulverization of Subgrade Soils in Preparation for Lime Treatment

<i>State</i>	<i>% Passing #4 Sieve</i>	<i>% Passing 2.5" Sieve</i>	<i>Additional Requirements</i>
<i>Arkansas</i>	<i><80 (Partially Pulverized)</i>		<i>Discard material retained on 3" sieve</i>
<i>Louisiana</i>	<i>50</i>		<i>Not required prior; required after stabilization</i>
<i>New Mexico</i>	<i>80</i>		<i>Discard material retained on 3" sieve</i>
<i>Oklahoma</i>		<i>75</i>	<i>Reduce material retained on 3" sieve until passing</i>
<i>Texas</i>		<i>100</i>	

2.2.3 Application of Stabilizing Agent

This section defines how to place the chemical stabilizer throughout the construction site. Variations between states other than Texas are negligible when it comes to applying and spreading cementitious stabilizer. Application of lime stabilizer, on the other hand, has some noticeable differences between states.

2.2.3.1 Application Requirements for Cement Treated Subgrades

Arkansas, Louisiana, New Mexico, and Oklahoma all require cementitious stabilizer to be applied dry. Texas, however, allows both dry and slurry stabilizer placement. Dry cement is typically poured via dump truck in specified amounts throughout the construction area. Approved spreading equipment then distributes the piles of cement evenly throughout the site. For the slurry method, cement and water are mixed

and continuously agitated in a slurry truck and then sprayed uniformly throughout the site until the design cement content is reached.

2.2.3.2 Application requirements for Lime Treated Subgrades

The five southern plains states allow lime stabilizer to be applied either dry or as a slurry. Dry lime products typically include quick lime and hydrated lime. They can both be distributed through the construction area with a spreading truck. Louisiana, Oklahoma, and Texas allow for hydrated lime to also be distributed in bags and then spread. Approved spreading equipment then distributes the piles of lime evenly throughout the site. For the slurry method, lime and water are mixed and continuously agitated in a slurry truck and then sprayed uniformly throughout the site until the design lime content is reached.

Uniformly spreading the chemical stabilizer presents unique challenges regarding spatial homogeneity. Due to the large scale nature of subgrade stabilization, spatial variability is anticipated. Uniform thickness of stabilizer throughout the site is simply not possible due to factors like surface roughness from scarification and tire depressions from the work trucks. Stabilizer will fill these depressions and voids, creating higher concentrations of stabilizer in those locations.

2.2.4 Mixing

This sub-section provides requirements on mixing the stabilizing agent with the prepared subgrade. Differences in procedures between states are negligible for cement mixing while some small difference exist for lime mixing.

2.2.4.1 Mixing requirements for Cement Treated Subgrades

All of the southern plains states require cement stabilizing agents to be mixed into the subgrade with self-powered mechanical rotor mixers as seen in Figure 2. All design specifications call for the site to be mixed until a uniform mix is achieved; however, Louisiana is only state that includes a minimum number of passes (i.e. two passes with the mixer). Each specification requires that moisture is continuously added during operations to maintain a moisture content that is at optimum or slightly higher than optimum and that mixing depth should be limited to the design depth of the subgrade.



Figure 2: Self-Powered Mechanical Rotor Mixers

2.2.4.2 Mixing Requirements for Lime Treated Subgrades

The mixing phase of lime treatment generally consists of an initial mixing phase, followed by a mellowing period, followed by a final mixing phase. Mixing is achieved using self-powered mechanical rotor mixers as seen in Figure 2, which must also be equipped to inject water while mixing. Arkansas and Oklahoma require a minimum mellowing time of three days, Louisiana requires two days, and New Mexico and Texas require one day. Final mixing is achieved by the same means as initial mixing.

Adequately mixing the chemical agents into the soil to produce a uniform mix is one of the most challenging components of subgrade stabilization (Army

and Air Force 1994). Inadequate mixing is defined in some design specifications as the presence of visible streaks and pockets of stabilizing agent. This is limited to the surface, however. Spatial and depth heterogeneity is likely inevitable due to the macro nature of mixing and the micro nature of chemical reactions. Additionally, it is unlikely that all stabilizer in the subgrade reacts completely with each of the constituents for the reaction (i.e. the soil and water).

2.2.5 Compaction

This section provides instructions on how to achieve proper soil compaction and homogenize the subgrade material in terms of density and moisture content throughout its design depth. There are small differences between states on these procedures as well as between compaction of lime and cement stabilized projects.

All southern plains states require subgrades to be compacted immediately after mixing to 95% of the maximum laboratory density. Cement treated subgrades are to be compacted immediately, while lime treated subgrades required a mellowing period, as discussed earlier. Maximum laboratory density, optimum moisture content, field density, and field moisture content are obtained in accordance with different publications throughout the region. These documents as well as differences in field moisture content limitations and maximum compaction time after cement mixing are all presented by state in Table 3. There are maximum compaction times for lime mixing. The only other notable difference in compaction specifications is that Louisiana requires sheepfoot or

tamping foot rollers for initial compaction. Pneumatic rollers are mentioned in all other specifications for compaction.

Table 3: Differences in Stabilization Specifications for Compaction of Subgrade Soils

<i>State</i>	<i>Max Lab Density / Optimum Moisture Content</i>	<i>Field Density Determined By</i>	<i>Field Moisture Content Determined By</i>	<i>Field Moisture Content Limitations</i>	<i>Maximum Compaction Time after Cement Mixing</i>
<i>Arkansas</i>	<i>AASHTO T 134</i>	<i>AASHTO T 310</i>	<i>AASHTO T 310</i>	<i>± 5% OMC</i>	<i>2 hours</i>
<i>Louisiana</i>	<i>DOTD TR 415 or 418</i>	<i>DOTD TR 436</i>	<i>DOTD TR 403</i>	<i>± 2% OMC</i>	<i>3 hours</i>
<i>New Mexico</i>	<i>AASHTO T 180</i>	<i>n/a</i>	<i>n/a</i>	<i>+ 3 to 5% OMC</i>	<i>4 hours</i>
<i>Oklahoma</i>	<i>AASHTO T 180</i>	<i>AASHTO T 310</i>	<i>AASHTO T 99</i>	<i>± 2% OMC</i>	<i>2 hours</i>
<i>Texas</i>	<i>TEX - 120 E</i>	<i>TEX - 115 E</i>	<i>TEX - 103 E</i>	<i>± 2 % OMC</i>	<i>2 hours</i>

In conclusion, there are plenty of opportunities to induce stabilizer distribution errors, both spatially and with depth, during subgrade stabilization. Due to the complex nature of soil, it is unrealistic to strive for a perfectly homogenous subgrade; however, it is not unreasonable to make efforts to mitigate these distribution errors to the best of our abilities. XRF spectrometry may be a valuable aid in this effort.

2.3 XRF Spectrometry

XRF spectrometry has been extensively studied for the better part of the last century. The works of Charles G. Barkla and Henry G.J. Moseley in the early 1900's laid

the foundation for this technology by identifying correlations between emitted radiation (i.e. fluorescence X-ray radiation) from samples subjected to X-rays and the chemical makeup of the samples (Moseley 1914; Moseley 1913; Barkla and Sadler 1909). These discoveries were built upon and eventually lead to the development of technologies capable of quantitatively determining the elemental composition of unknown samples. The XRF industry flourished after the 1950s and continues to flourish today, finding its place in dozens of industries for countless applications. Some of these applications include environmental analyses of water quality, air quality, and lead contamination (Abdelbagi, et al. 2011; Binstock, et al. 2008; Kim, et al. 2007; Zawisza and Sitko 2006); pharmaceutical analyses of drug impurities, catalyst residues, and vitamin extraction (Moradi, et al. 2015; Ortiz, et al. 2012; Arzhantsev, et al. 2011; Marguá, et al. 2009); archeological analyses of obsidian (Frahm 2013; Forster and Grave 2012; Millhauser, et al. 2011); and consumer goods analyses of FDA-regulated products and household items (Sun, et al. 2013; Kulikov, et al. 2012; Palmer, et al. 2009) to name a few. PHXRF has further transformed these industries by providing the benefits of accurate, non-destructive analysis capabilities with the convenience of portability, saving time and sample transport and storage costs (Parsons, et al. 2013).

PHXRF conveniently equips the user with a handheld elemental analysis tool that can determine the makeup of a material in as little as 30 seconds. A description of the testing process after engaging the trigger is as follows. The devices activate a rhodium target X-ray tube which generates a uniform stream of X-rays. These X-rays pass through the soil sample, ejecting electrons in the lower level orbitals along the way, similarly to what is illustrated in Figure 3. This creates an unstable atom. The electrons on the outer

orbitals of the atom then “jump” down to fill the void of the ejected electron. This “jump” requires the electrons to go from a higher energy states to a lower ones; that is to say, the electrons emit energy during this jump. This energy is in a form of radiation called X-ray fluorescence, which is unique to the atom that it comes from. The handheld devices have a 10 mm² silicon drift detector that identifies this radiation. The onboard computer converts these readings into elemental percentages by weight or ppm.

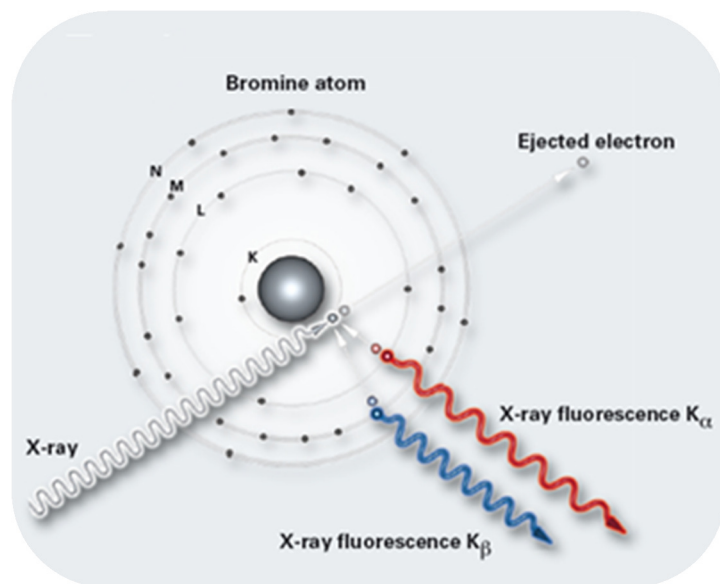


Figure 3: XRF Emitted from a Radiated Bromine Atom (Bruker 2013)

Extensive research focusing on XRF sample preparation has been conducted over the years. The literature suggests that soil preparation is particularly challenging due to the complex and non-homogenous nature of the material; but, these challenges can be mitigated with appropriate preparation techniques and analysis. Many errors are dependent on the type of XRF sample that is prepared. For this research, pressed pellets and powder samples were created. Pressed pellets often fall victim to systematic errors,

such as absorption and enhancement (Parsons, et al. 2013; Imanishi 2010), variations in chemical states, and particle size effects (Hürkamp, et al. 2009; Kruskerski 2006).

Absorption is an effect caused by the presence of water. Water easily absorbs low energy X-rays, so its presence will degrade detectability (Imanishi 2010). For optimal measurements, water content should be as low as possible (Imanishi 2010). This effect is more pronounced in fine soils and is often underestimated in the literature (Parsons, et al. 2013). For this experiment, all mixes were air dried to reduce these effects.

Particle size effects, which are typically the most significant source of error for pressed pellets, affect the intensities of XRF that are emitted from the sample (Kruskerski 2006). When larger particle sizes are present, XRF intensities are typically weaker, particularly in lighter elements such as calcium (Maruyama 2008). XRF intensities decrease as the distance from the radiated atom to the XRF detector increases (Imanishi 2010). In samples with larger particles, larger voids are present which increases this distance as seen in Figure 4 (Imanishi 2010). These effects occur in granular materials and can be reduced but not totally eliminated by homogenizing the sample (Markowicz 2011). For this study, a variety of particle sizes were tested to determine the necessary amount of milling required to achieve PHXRF *SC* measurements comparable to the measurements of commercial laboratory.

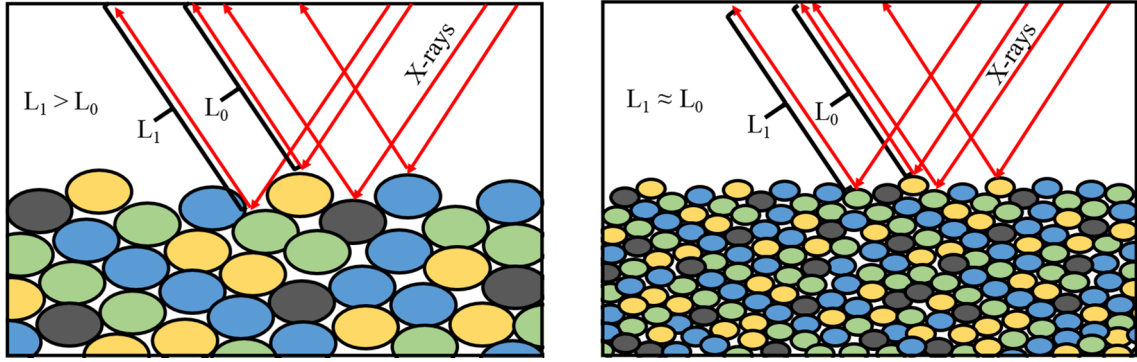


Figure 4: Effect of Particle Size on Length of XRF Path

For XRF applications specific to stabilized subgrades, previous research validated that commercialized laboratory XRF produce accurate and reliable results when used to determine SC in subgrade soils (Cerato and Miller 2013). It was found that the “Whole Rock Analysis” method conducted by ALSglobal laboratories is accurate to within 0.01% when determining calcium oxide content in four different soils mixed with three different stabilizers (Cerato and Miller 2013). These conclusions were drawn from several blind trials over a four year period (Cerato and Miller 2013). The “Whole Rock Analysis” method subjects the sample to meticulous sample preparation. After milling, the samples are fused into glass discs, which effectively eliminates moisture and particle size effects. SC can be calculated from the calcium oxide contents, CaO , of the stabilized soil, raw soil, and chemical additive using Equation (1). All SC s presented in this research were calculated using this equation.

$$SC = \left[\frac{CaO_f - CaO_0}{CaO_{CA} - CaO_0} \right] \times 100\% \quad (1)$$

Where: CaO_f = *CaO measured by XRF in the chemically stabilized soil sample (%)*

CaO_0 = *CaO measured by XRF in the untreated natural soil sample (%)*

CaO_{CA} = *CaO measured by XRF in the chemical additive (%)*

The aforementioned research led to this current investigation to verify that PHXRF systems have accuracy comparable to those of commercial laboratories.

CHAPTER 3

METHODS

3.1 Materials and Apparatuses

The materials, including soil and stabilizer type, and non-standard laboratory equipment used in this research are as follows:

- *Old Hickory Clay (OHC)* – Kaolinite soil from Hickory, Kentucky
- *Super Gel-X Bentonite (SGB)* – Absorbent impure bentonite clay from Titan Industries Inc.
- *Hydrated Lime* – Quicklime and water mix from the Texas Lime Company in Cleburne, Texas.
- *Cement Kiln Dust (CKD)* – Fine, highly alkaline waste removed from cement kiln exhaust from Silver Star Construction Co., Inc. in Moore, Oklahoma
- *Fly Ash Class C* – Fine residue generated in combustion from Silver Star Construction Co., Inc. in Moore, Oklahoma
- *SPEX Shatterbox 8515* – Fully automated electric miller
- *SPEX 3630 X-Press* – Automatic press machine used to press pellet samples
- *SPEX 40mm Evacuatable Die Set* – Die set used to create pressed pellets
- *Premier Lab Supply 40mm Tapered Wall Aluminum Cups* – Shallow, thin-walled aluminum caps for reinforcing pressed pellets
- *Premier Lab Supply PB-100 Binding Additive* – Cellulose powder used to bond materials together in pressed pellet samples

- *Premier Lab Supply 35mm Single Open Ended Cup/Ring/Collar* – Sample cup used for powder samples
- *Premier Lab Supply Mylar Low Sulfur Pre-Cut Thin Film* – Film used on the scanning surface of the powder samples
- *Bruker S1 Titan* – PHXRF spectrometer
- *Thermo Scientific Niton XL3t GOLDD+* – PHXRF spectrometer

3.2 Testing Matrix

3.2.1 Laboratory

Two different one-mineral soils, OHC and SGB, were combined with various amounts of hydrated lime, CKD, and fly ash to create 14 mixes with *SCs* ranging from 0 to 64%. These 14 mixes were milled to particle diameters of passing the No. 4, No. 40, No. 100, and No. 200 sieves, creating a matrix of 56 total samples. A portion of these samples were pressed into 56 compacted pellets and a portion of the passing No. 200 sieve samples were used to create 14 powder samples. This created a total matrix of 70 samples of varying *SCs*, particle sizes, and sample types. This matrix, along with the corresponding number of scans per unique sample by two PHXRF spectrometers, is illustrated in Table 4. A variety of analysis techniques were assessed including scan duration and standard or quartering scan techniques. Finally, the results of these devices were compared to results received from a commercial laboratory in order to determine the most practical, effective, and accurate preparation and analysis techniques. Device

recommendations were made based on the performances of the PHXRF spectrometers.

Table 4: Testing Matrix Showing Number of Scans (S1 Titan / Niton XL3t) of all Seventy Unique Samples and their Corresponding Soil Types, Stabilizer Contents, Sample Types, and Maximum Particle Sizes

	Stabilizer Content (%)	Pressed Pellets				Powder
		Passing No. 4	Passing No. 40	Passing No. 100	Passing No. 200	Passing No. 200
OHC	0 Raw	40 / 3	40 / 3	40 / 3	40 / 3	52 / 15
	4 Lime	40 / 3	40 / 3	40 / 3	40 / 3	52 / 15
	7 Lime	40 / 3	40 / 3	40 / 3	n/a	n/a
	15 CKD	40 / 3	40 / 3	40 / 3	40 / 3	52 / 15
	23 CKD	40 / 3	40 / 3	40 / 3	40 / 3	52 / 15
	44 Fly Ash	40 / 3	40 / 3	40 / 3	40 / 3	52 / 15
	64 Fly Ash	40 / 3	40 / 3	40 / 3	40 / 3	52 / 15
SGB	0 Raw	12 / 3	12 / 3	12 / 3	12 / 3	24 / 15
	4 Lime	12 / 3	12 / 3	12 / 3	12 / 3	24 / 15
	6 Lime	12 / 3	12 / 3	12 / 3	12 / 3	24 / 15
	12 CKD	12 / 3	12 / 3	12 / 3	12 / 3	24 / 15
	21 CKD	12 / 3	12 / 3	12 / 3	12 / 3	24 / 15
	41 Fly Ash	12 / 3	12 / 3	12 / 3	12 / 3	24 / 15
	63 Fly Ash	12 / 3	12 / 3	12 / 3	12 / 3	24 / 15

3.2.2 Field Testing

Three different subgrade stabilization sites with different calcium-based stabilizers were located throughout the state of Oklahoma. Both in situ and ex situ PHXRF measurements were taken at each site in a grid pattern over a 50 foot long by 10 foot wide area. In situ measurements are defined in this thesis as taking

surface PHXRF measurements at the grid locations with no sample preparation. Ex situ measurements, on the other hand, are defined as retrieving soil samples from the 33 grid locations, bringing them back to the laboratory, processing them over a #40 sieve, placing them in sample cups, and using the PHXRF to measure SC. PHXRF measurements and samples were taken every five feet along the length and width of the area for a total of 33 locations. This allowed for spatial homogeneity to be assessed. At the 33 locations, samples were taken at various depths as well. For pre-treatment samples, 0 - 9 inch and 9 - 12 inch samples were taken; for post-treatment samples, 0 - 3 inch, 3 - 6 inch, 6 - 9 inch, and 9 - 12 inch samples. This allowed for depth homogeneity to be assessed. Additionally, random grid samples were analyzed by a verified commercial laboratory to assess field accuracy of the PHXRF device.

3.3 Mixing Procedures

The moisture content of the soils, w_c , were determined for OHC and SGB soils in accordance with ASTM D2216-10 Standard Test Methods for Laboratory Determination of Water (Moisture) Content of Soil and Rock by Mass prior to mixing with stabilizer. Amounts of soil and chemical stabilizer required to produce a wide range of SCs by dry mass were calculated using Equations (2) and (3). SCs chosen for this experiment stretch from 0 to 64% in order to assess the limits of the PHXRF units for the applications mentioned earlier in this research. Table 5 presents the calculated amounts of the soils and stabilizers needed to produce 14 mixes that span this range.

$$M_{Stab} = \frac{SC \times M_{Total}}{100\%} \quad (2)$$

Where: M_{Stab} = total mass of chemical stabilizer in sample (Note: moisture \approx 0%) (kg)

M_{Total} = total dry mass of sample (kg)

S_c = percentage of sample that is chemical stabilizer (i.e. $S_c = \frac{W_{Stab}}{W_{Total}} \times 100\%$) (%)

$$M_{Soil} = \frac{M_{Total} \left(1 - \frac{S_c}{100\%}\right)}{\left(1 - \frac{w_c}{100\%}\right)} \quad (3)$$

Where: M_{Soil} = total mass of soil in sample (Note: including moisture) (kg)

M_{Total} = total dry mass of sample (kg)

S_c = percentage of sample that is chemical stabilizer (i.e. $S_c = \frac{W_{Stab}}{W_{Total}} \times 100\%$) (%)

w_c = water content of soil (%)

Table 5: Proportions of Soil and Stabilizer to Achieve a Range of Stabilizer Contents

	Sample Name	SC (%)	w_c (%)	M_{Total} (kg)	$M_{Stabilizer}$ (kg)	M_{Soil} (kg)
OHC	Raw	0.00	1.2	2	0.000	2.024
	4 Lime	4.21	1.2	2	0.084	1.939
	7 Lime	7.10	1.2	2	0.142	1.881
	15 CKD	15.1	1.2	2	0.302	1.719
	23 CKD	22.7	1.2	2	0.454	1.565
	44 Fly Ash	43.8	1.2	2	0.876	1.138
	64 Fly Ash	64.3	1.2	2	1.286	0.723
SGB	Raw	0.00	6.4	2	0.000	2.137
	4 Lime	3.72	6.4	2	0.074	2.057
	6 Lime	6.28	6.4	2	0.126	2.003
	12 CKD	12.5	6.4	2	0.250	1.870
	21 CKD	20.6	6.4	2	0.412	1.697
	41 Fly Ash	40.9	6.4	2	0.818	1.263
	63 Fly Ash	63.1	6.4	2	1.262	0.788

The samples were dry mixed in the quantities presented in Table 5 to reduce the amount of stabilizer agglomerations that would form after water was added. For OHC samples, 3000mL of tap water was added to induce pozzolanic reactions and to produce a highly workable mix. For SGB sample, 8000mL of tap water was added for the same reasons. SGB required significantly more water because it is a highly expansive montmorillonite clay with more absorptive properties. All samples were mixed for five minutes using a mechanical blender with a wire whisk attachment as seen in Figure 5.



Figure 5: Mixing Samples with a Mechanical Blender

After blending, the mixes were air dried for two to four weeks. It was important that the samples were not oven dried. This was because kaolinite disintegrates at

temperatures near 550°C (Insley and Ewell 1935). Once dry, a sample of each of these mixes was mailed to ALSglobal where it was subjected to a whole rock analysis to determine the CaO content in each sample. Their CaO determinations were converted into *SC*s using Equation (1) and were used as true *SC* values for the purposes of this research.

3.4 Milling Procedures

The six OHC mixes, six SGB mixes, and two “raw” samples (i.e. samples with not stabilizer additives) were all subjected to different sample preparation regiments in order to assess the effects of several variables on the precision and accuracy of the PHXRF devices. Milling rigor was the first of these variables to be introduced.

It is important to note that creating a matrix of samples with different particle sizes is not as straightforward as performing a standard sieve analysis and creating samples from the material retained in each sieve. Doing so would producing samples that consists of different proportions of coarse and fine fractions (e.g. passing No. 4 sample would primarily consist of coarse material, passing No. 200 sample would primarily consist of fine material). These samples would therefore contain different minerals and elements, making it impossible to assess the effects of milling efforts on accuracy. Instead, the mixes in this experiment underwent the following treatment. The mixes were ground using a SPEX Shatterbox 8515, as seen in Figure 6, until all material passed the largest sieve (i.e. passing the No.4 sieve). A portion of this result was retrieved for the Passing No. 4 samples and the remainder underwent further milling until all material passes the next largest sieve (i.e. passing No. 40 sieve). A portion of this result was retrieve for the

passing No. 40 samples, etc. This was completed for sieve sizes of No. 4, No. 40, No. 100, and No. 200, thus making samples of identical minerals and elements but different particle diameters. Sieve agitation was achieved via a Humboldt Sieve Shaker for 10 minute periods. The retrieved samples of various particle diameters were bagged and marked according the material contained within.



Figure 6: SPEX Shatterbox 8515 Used to Mill Samples

3.5 Pressed Pellet Procedures

Each of the 56 unique bagged sample materials was processed into pressed pellets for XRF analysis. For OHC samples, eight grams of the sample material and two grams of Premier Lab Supply PB-100 Binding Agent were dry mixed together. The binding agent is an organic compound added to increase cohesion in the soil. It is comprised of elements that are too light to be detected by XRF spectrometry; therefore, its effect on the measurements in this experiment are assumed to be negligible. The dry mix of sample material and binder was transferred to a SPEX Evacuatable Die Set, as seen in Figure 7.

The die set was subjected to 25,000 lbs. of pressure for 60 seconds to produce a compacted pellet of material. The SGB samples underwent a similar process with the only difference being the proportions of mixed material and binder. For the SGB samples, 14 g of soil and 1.4 g of binder were mixed. The bottom of each pellet was marked according to the material that it was comprised of.



Figure 7: Removing Plunger from SPEX Evacuatable Die Set

3.6 Powder Sample Procedures

Of the passing No. 200 sieve materials, 14 total powder samples were created: 7 OHC samples of varying *SC* and 7 SGB samples of varying *SC*. This brought the total matrix of samples to 70: 56 pressed pellets and 14 powder samples.

Creating a powder sample required very little effort. A Premier Lab Supply sample cup was filled to the top with the aforementioned milled material. A piece of

Premier Lab Supply Mylar film was secured over the opening of the cup with a sample ring, as seen in Figure 8.



Figure 8: XRF Powder Sample

It is very important to fill the sample cups completely to the top with sample material. If too little material is placed inside, then a gap will develop between the surface of the material and the film. This gap adversely affects the accuracy of the PHXRF measurements, especially in lighter elements like calcium, by elongating the XRF path between the material and the detector of the device. Observe the difference between a poorly prepared powder sample and an adequately prepared powder sample in Figure 9.



Figure 9: Poorly Prepared Powder Sample (Left) and Adequately Prepared Powder Sample (Right)

3.7 Laboratory Testing of PHXRF

A Bruker S1 Titan and a Thermo Scientific Niton XL3t GOLDD+ were used to analyze the 70 sample matrix. Both the S1 Titan and Niton XL3t were set to their respective factory-installed soil calibrations for the analyses. These devices can be seen in Figure 10. It should be noted that X-ray radiation is emitted from the nose of these devices, which can cause serious injury if improperly used. Safety training and instrument familiarization is imperative before handling.



Figure 10: (Left) Bruker S1 Titan in Desktop Stand and (Right) Thermo Scientific Niton XL3t GOLDD+ in Field Stand

Effects of scan durations and scan techniques were assessed on the S1 Titan. The S1 Titan is equipped to perform dual phase measurements. Phase I detects the light elements of Mg, Al, and Si, and Phase II detects non-light elements. Since calcium is the element central to this research, Phase II scan durations were varied to longer lengths. The following scan durations were assessed: 30 - 30, 15 - 45, 15 - 60, and 15 - 120, where the first number represents the length of Phase I scan in seconds and the second number represents Phase II. The effects of scan durations on *SC* precision and accuracy were monitored. All measurements with the Niton XL3t were limited to 60 seconds because longer scan durations produced no meaningful benefits for the S1 Titan measurements. Scan technique was assessed by conducting standard scans (i.e. scanning a sample three times in the same place) and quartering scans (i.e. scanning the first quadrant three times,

rotating it 90°, scanning the second quadrant three time, rotating it 90°, etc.) on all powder samples with both the S1 Titan and the Niton XL3t. Quartering of samples is illustrated in Figure 11. This technique was used to assess sample homogeneity.

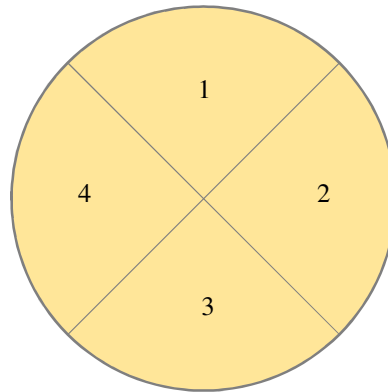


Figure 11: Dividing Powder Samples into Four Quadrants

3.8 Laboratory Testing Data Analysis

The effects of four variables (i.e. scan duration, particle size, sample type, and scan technique) on the precision and accuracy of the PHXRF devices were analyzed. Precision of the devices was assessed using standard deviation (STDEV), coefficient of variation of the standard deviation (COV_{STDEV}), and linear regression. STDEV is a statistics method used to quantify the variation between each discrete *SC* measurement and the mean *SC* value of the group of measurements. High precision is indicated by a STDEV that is close to zero. COV_{STDEV} is used to assess the dispersion of the discrete *SC* measurements to the mean *SC* value. It is defined as the ratio between the STDEV and the mean. High precision is indicated by a COV_{STDEV} close to zero. Linear regression is a statistics method used to quantify the strength of the relationship between the discrete

SC measurements and the combined trendline of the sample. High precision is indicated by an R^2 value close to one.

The accuracy of the PHXRF devices was assessed using root-mean-square deviation (RMSD), coefficient of variation of the root-mean-squared deviation (COV_{RMSD}), and linear regression. RMSD is a statistics method used to quantify the variation between each discrete *SC* measurement and a true *SC* value of a sample. High accuracy is indicated by a RMSD that is close to zero. COV_{RMSD} is used to assess the dispersion of the discrete *SC* measurements to the true *SC* value. High accuracy is indicated by a COV_{RMSD} that is close to zero. Linear regression can be used to assess accuracy in addition to precision. This was done by comparing the combined trendline of the measurement data set for a unique sample to a $y = x$ line. A $y = x$ line would indicate a perfect match between measured and true *SC* values of the sample; therefore, a trend line close to $y = x$ would indicate high accuracy.

3.9 Field Testing of PHXRF

Three highway subgrade stabilization projects were located locally in the state of Oklahoma. Locations of the sites are illustrated in Figure 12. Site 1 was a CKD stabilization project on a temporary collector road on Interstate 35 southbound ($35^{\circ}12'10.22''N$, $97^{\circ}28'48.11''W$). It was stabilized to a *SC* of 15% on 5 June 2015. Site 2 was a fly ash stabilization project of a four lane section of the Route 9 and Interstate 35 interchange ($35^{\circ}11'56.30''N$, $97^{\circ}29'0.42''W$). It was stabilized to a *SC* of 16% on 11 June 2015. Site 3 was a Portland cement stabilized project south of Main Street on the southbound lanes of Interstate 35 ($35^{\circ}11'53.69''N$, $97^{\circ}28'53.55''W$). It was stabilized a

SC of 10% on 16 September 2015. These sites were subjected to a pre- and post-treatment field sampling and testing program in order to assess spatial and depth heterogeneity. Three methods were used to analyze the samples from these sites: an in situ analysis, a laboratory analysis with minimal sample preparation, and an external analysis by a verified commercial laboratory (i.e. ALSglobal).



Figure 12: Locations of Field Test Sites 1, 2, and 3

The in situ measurements were taken in a grid pattern to assess spatial variability in the site. A 10 foot wide by 50 foot long grid was marked on the sites in 5 foot increments (i.e. 3 locations across the width and 11 locations down the length) for a total of 33 testing locations. A diagram of the measurement grid is illustrated in Figure 13.

Three 30 second in situ measurements were taken with the Niton XL3t PHXRF device at each of the locations. Prior to scanning, the scan locations were mildly tamped to provide a flat scanning surface.

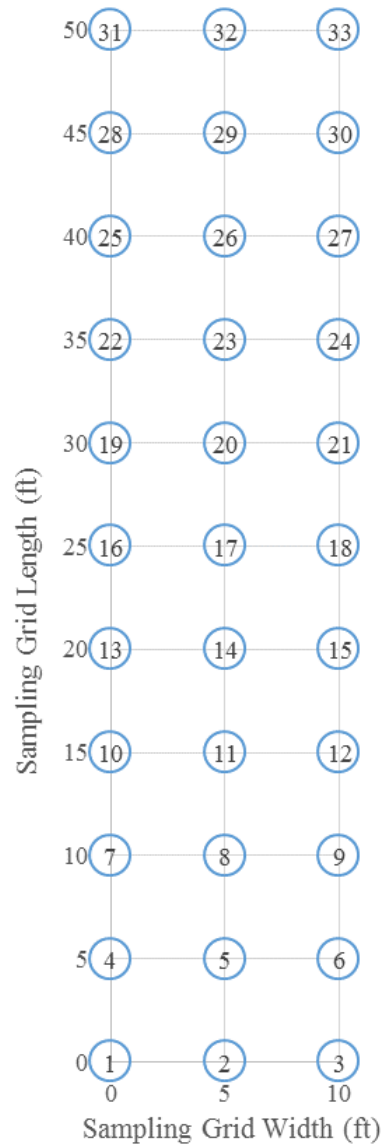


Figure 13: Spatial XRF Testing and Sampling Locations in the Field

Samples were also retrieved from each of the 33 scanned locations for ex situ testing to further assess spatial homogeneity. Ex situ samples were brought back to the laboratory, processed over a #40 sieve, placed into sample cups, and measured with PHXRF for *SC* content. These ex situ samples were taken to a depth of 12 inches to assess depth homogeneity. Since subgrades are typically stabilized to a depth of 8 inches, sampling to a depth of 12 inches allowed for verification that the target depth was achieved and verification that the soil below 8 inches was not treated. These 12 inch deep samples were divided into two pre-treatment subdepths (i.e. 0 - 9 inches and 9 - 12 inches) and four post-treatment subdepths (i.e. 0 - 3 inches, 3 - 6 inches, 6 - 9 inches, and 9 - 12 inches). Samples were retrieved using a hammer head soil probe, as seen in Figure 14, and taken to the laboratory. They were then passed through a No. 40 sieve and processed into powder samples. This type of sample preparation was chosen based on the particle size study that showed no appreciable increase in accuracy when soil was milled beyond the #40 and the sample type study that showed minimal differences in accuracy between pressed pellet and powder samples. Additionally, this type of sample preparation is exceedingly efficient and easily implementable in the field. Ex situ samples were scanned for 30 seconds each with the Niton XL3t.



Figure 14: Hammer Head Soil Probe Used to Retrieve Samples at Various Depths

3.10 Field Testing Data Analysis

In situ and ex situ SC measurements were assessed for precision and accuracy in the same manner as the laboratory samples (i.e. $STADEV$, COV_{STADEV} , $RMSD$, COV_{RMSD} , and linear regression). Spatial stabilizer homogeneity of the three stabilized sites was assessed using 2D contour graphs. These graphs illustrate plan views of the sites and variations in SC by color intensities. Depth stabilizer homogeneity was assessed in the same manner except from cross-section views of the sites. Additionally, depth homogeneity was studied using average SC versus depth graphs.

CHAPTER 4

RESULTS AND DISCUSSIONS

4.1 Introduction

The results of the both laboratory and field testing are presented in this chapter. The analyses of independent variables and their effects on precision and accuracy of the PHXRF devices are illustrated and discussed. Additionally, analyses of PHXRF field accuracy and deployment feasibility are presented and discussed as well as spatial and depth stabilizer distribution assessments.

4.2 PHXRF Laboratory Testing

The effects of several independent variables, including scan duration, scan technique, particle size, and sample type, on the precision and accuracy of the two PHXRF devices are presented. The effects of scan durations are presented only for the S1 Titan, whereas the effects of all other independent variables are presented for both the S1 Titan and the Niton XL3t. Accuracy of the PHXRF measurements is the primary focus of this research. While precision of the devices is important, it will only be elaborated on in cases where it affects the overall accuracy.

4.2.1 Scan Durations

Scan durations are found to have very little effect on the *SC* measurements for the S1 Titan. Though longer scan durations do tend to decrease STDEV and

increase RMSD, the lack of variability in the COV_{STDEV} and COV_{RMSD} prove that these differences are insignificant.

The results of the scan duration analysis for OHC samples are presented in Table 6. The insignificance of the variability in STDEV and RMSD can best be explained through an example. If the mean value of a series of *SC* measurements is 21.983%, then scanning the samples for 60 seconds (30 - 30) or 135 seconds (15 - 120) would yield measurements of $21.983 \pm 0.039\%$ or $21.983 \pm 0.021\%$, respectively. There is very little difference between these two values. This suggests that longer scan durations are inefficient because they yield no appreciable improvement in measurement repeatability. All observed scan durations in this research, regardless of length, produced remarkably repeatable results, which is indicated by the low COV_{STDEV} . Therefore, lengthening scan durations is unnecessary. Similar conclusions are drawn about accuracy via RMSD. For example, if the true *SC* of a sample is 22.456%, then scanning the samples for 60 seconds (30 - 30) or 135 seconds (15 - 120) would produce a measurements of $22.456 \pm 0.850\%$ or $22.456 \pm 0.876\%$. These changes are miniscule and, in this case, detrimental to PHXRF accuracy.

Table 6: Effects of Scan Duration on $STDEV$, COV_{STDEV} , $RMSD$,
and COV_{RMSD} for OHC Samples

Scan Durations sec (Phase I - Phase II)	n	$STDEV$ %	COV_{STDEV}	$RMSD$ %	COV_{RMSD}
60 (30-30)	270	0.039	0.002	0.850	0.069
60 (15-45)	270	0.027	0.001	0.851	0.069
75 (15-60)	270	0.034	0.001	0.875	0.069
135 (15-120)	270	0.021	0.001	0.876	0.070

The results from the SGB samples, which can be seen in Table 7, agree with those of the OHC samples. $STDEV$ and $RMSD$ increase and decrease slightly; however, the COV_{STDEV} and COV_{RMSD} show that these variations are negligible relative to the mean and true SC , respectively. The SGB samples support the OHC findings that longer scan durations are not only inefficient, but hinders the accuracy of PHXRF SC measurements.

Table 7: Effects of Scan Duration on $STDEV$, COV_{STDEV} , $RMSD$,
and COV_{RMSD} for SGB Samples

Scan Durations sec (Phase I - Phase II)	n	$STDEV$ %	COV_{STDEV}	$RMSD$ %	COV_{RMSD}
60 (30-30)	84	0.031	0.001	2.691	0.187
60 (15-45)	84	0.030	0.001	2.708	0.188
75 (15-60)	84	0.039	0.001	2.700	0.188
135 (15-120)	84	0.024	0.001	2.693	0.188

Linear regression analyses were used to examine the statistical significance of the differences between various scan durations. The results are

illustrated in Figure 15 and Figure 16 for the OHC and SGB samples, respectively. Regression line (a) is produced from all 60 second (30 - 30) scans, (b) is produced from all 60 second (15 - 45) scans, etc. Notice that there is virtually no difference between the four regression lines, further proving that longer scan durations are of little to no benefit. Furthermore, the bounds of the confidence intervals, which the mean of each set of measurements is 95% likely to fall in between, encompass all of the combined trend lines of each of the four scan durations tested. This infers that scan durations are not statistically significant enough to be a variable of concern. This trend is observed for both OHC and SGB samples.

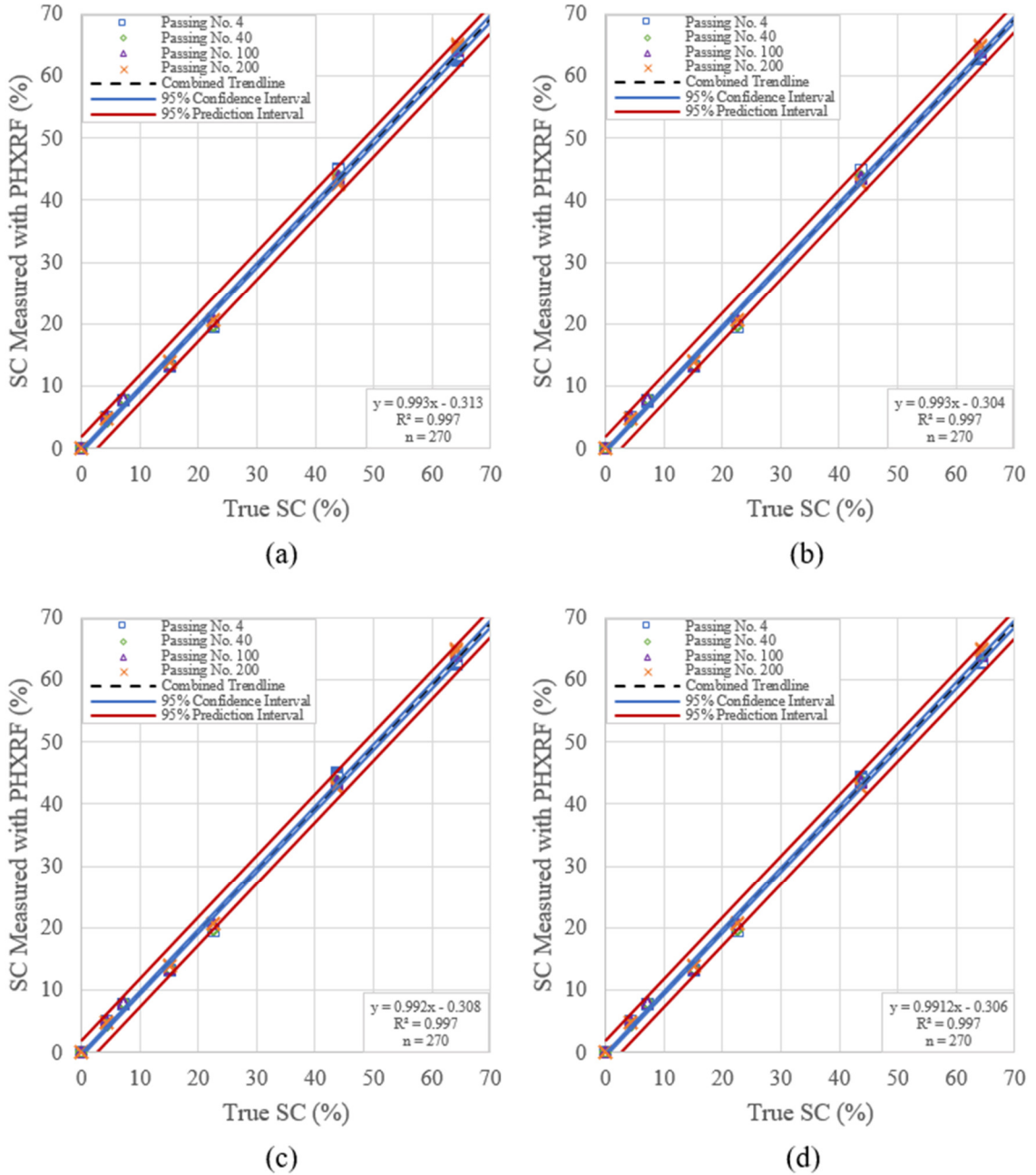


Figure 15: Effects of Various Scan Durations on Precision and Accuracy of S1 Titan PHXRF Device for (a) 60 Second (30 - 30), (b) 60 Second (15 - 45), (c) 75 Second (15 - 60), and (d) 135 Second (15 - 120) Scan Durations on OHC samples.

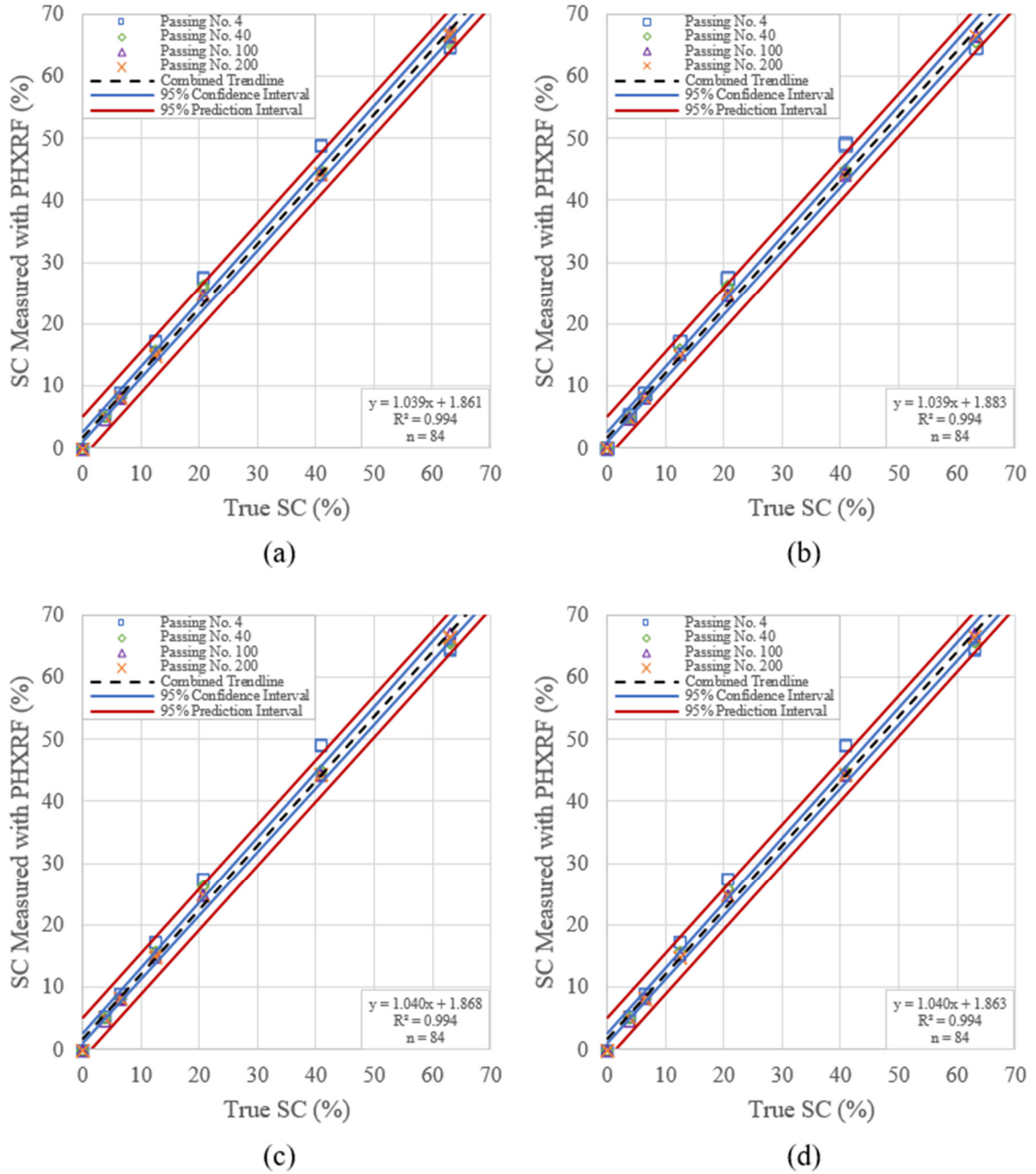


Figure 16: Effects of Various Scan Durations on Precision and Accuracy of S1 Titan PHXRF Device for (a) 60 Second (30 - 30), (b) 60 Second (15 - 45), (c) 75 Second (15 - 60), and (d) 135 Second (15 - 120) Scan Durations on SGB samples.

4.2.4 Scan Technique

Scan technique appears to play a sizable role in the precision of PHXRF *SC* measurements, but little to no role regarding accuracy. Disparities in precision are more pronounced in S1 Titan measurements as opposed to Niton XL3t ones. Accuracy was hardly affected, and no clear trends are able to be drawn from the data.

As seen in Table 8, scanning powder OHC samples with a standard technique as opposed to a quartering technique yields significant benefits with regards to precision for the S1 Titan. $STDEV$ decreases by 0.225% as a result, which is the most substantial change in $STDEV$ observed in this research. The large change in COV_{STDEV} for the S1 Titan prove the significance of this increase in precision. In contrast, $RMSD$ is barely affected by different scan techniques. Only small differences in the second and third decimal places of the $RMSD$ are observed.

Table 8: Effects of Scan Technique on $STDEV$, COV_{STDEV} , $RMSD$, and COV_{RMSD} for OHC Samples

	<i>Scan Technique</i>	<i>n</i>	<i>STDEV (%)</i>	<i>COV_{STDEV}</i>	<i>RMSD (%)</i>	<i>COV_{RMSD}</i>
<i>S1 Titan</i>	<i>Standard</i>	240	0.029	0.001	2.153	0.133
	<i>Quartering</i>	72	0.254	0.015	2.172	0.140
<i>Niton XL3t</i>	<i>Standard</i>	18	0.099	0.005	2.800	0.096
	<i>Quartering</i>	72	0.108	0.006	2.802	0.104

The results from the SGB samples agree with those of the OHC samples in terms of precision. These results can be seen in Table 9. Once again, precision is heavily influenced by scan technique for the S1 Titan measurements but not for the Niton XL3t. Accuracy is affected by scan technique for the SGB samples, which conflicts with the findings of the OHC samples. When using a standard scanning technique, RMSD is improved by 0.158% for the S1 Titan but worsened by 0.103% for the Niton XL3t. Since these results conflict with one another and the results from the OHC samples, the effects of scan technique on the accuracy of PHXRF *SC* measurements is deemed inconclusive.

Table 9: Effects of Scan Technique on STDEV, COV_{STDEV}, RMSD, and COV_{RMSD} for SGB Samples

	<i>Scan Technique</i>	<i>n</i>	<i>STDEV (%)</i>	<i>COV_{STDEV}</i>	<i>RMSD (%)</i>	<i>COV_{RMSD}</i>
<i>S1 Titan</i>	<i>Standard</i>	84	0.035	0.002	1.808	0.145
	<i>Quartering</i>	84	0.108	0.006	1.966	0.142
<i>Niton XL3t</i>	<i>Standard</i>	21	0.068	0.004	0.980	0.051
	<i>Quartering</i>	84	0.099	0.005	0.877	0.039

An interesting observation in these results is the large difference in precision between the two techniques for the S1 Titan but not for the Niton XL3t. The S1 Titan results seem to suggest that the soil samples were not uniform. As

the sample was rotated and scanned, the measurements varied greatly, far greater than scanning the sample repeatedly in one location. This observation was not confirmed by the Niton XL3t results, however. The explanation for this phenomenon may be that the footprint of the x-ray beam emitted from the S1 Titan is ellipse shaped and has an area of 15.71 mm². The footprint of the Niton XL3t's x-ray beam, on the other hand, is more than three times larger. It is circular and has an area of 50.27 mm². These beam profiles can be seen in Figure 22. This suggests that measurements taken by the Niton XL3t are naturally more of an average of the sample than those of the S1 Titan because of the significantly larger beam footprint. Therefore, it makes sense that the Niton XL3t found less variation throughout the sample as compared to the S1 Titan.



*Figure 17: Beam Footprints of the S1 Titan (Left) and Niton XL3t
(Right) PHXRF Devices*

The linear regression analyses verify the statistical significance of the effects of scan technique on PHXRF measurements. The results of the OHC and SGB measurements for the S1 Titan are illustrated in Figure 18 and Figure 20; for the Niton XL3t, Figure 19 and Figure 21. Notable variations in the equations of the regressions lines are observed, both in terms of the slopes and the y-intercepts. The variations are large enough to place the combined trendlines outside of the 95% confidence intervals of the correlating graphs, which verifies the statistical significance of the effects of scan technique on accuracy of the PHXRF devices. Additionally, accuracy of the PHXRF devices is illustrated in these figures by the closeness of the combined trendlines to a $y = x$ line. In most cases, the standard scan technique produces more accurate and more precise measurements, except in the case of the quartering scans of the SGB samples with the Niton XL3t as explained earlier.

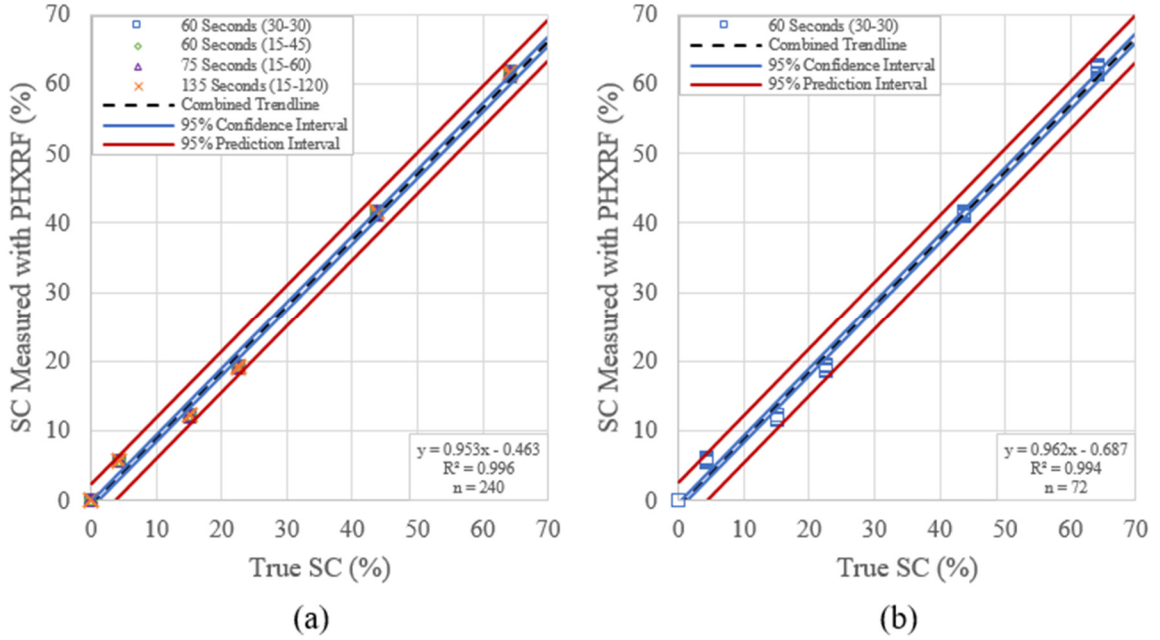


Figure 18: Effects of (a) Standard and (b) Quartering Scan Techniques on Precision and Accuracy of S1 Titan PHXRF Device for OHC Samples.

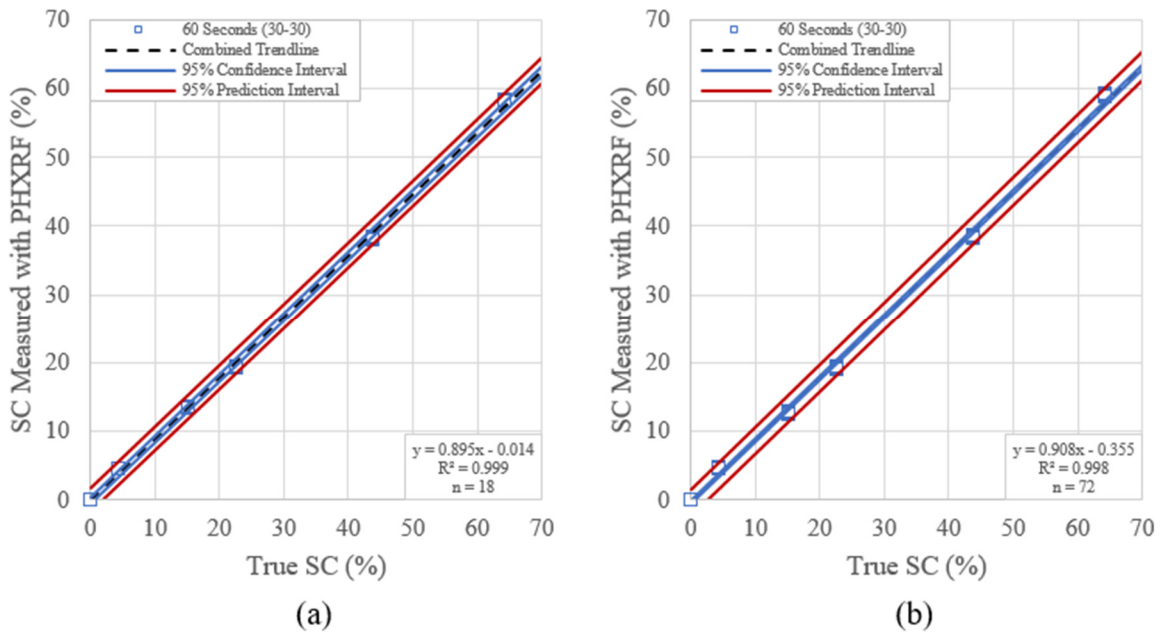


Figure 19: Effects of (a) Standard and (b) Quartering Scan Techniques on Precision and Accuracy of Niton XL3t PHXRF Device for OHC Samples.

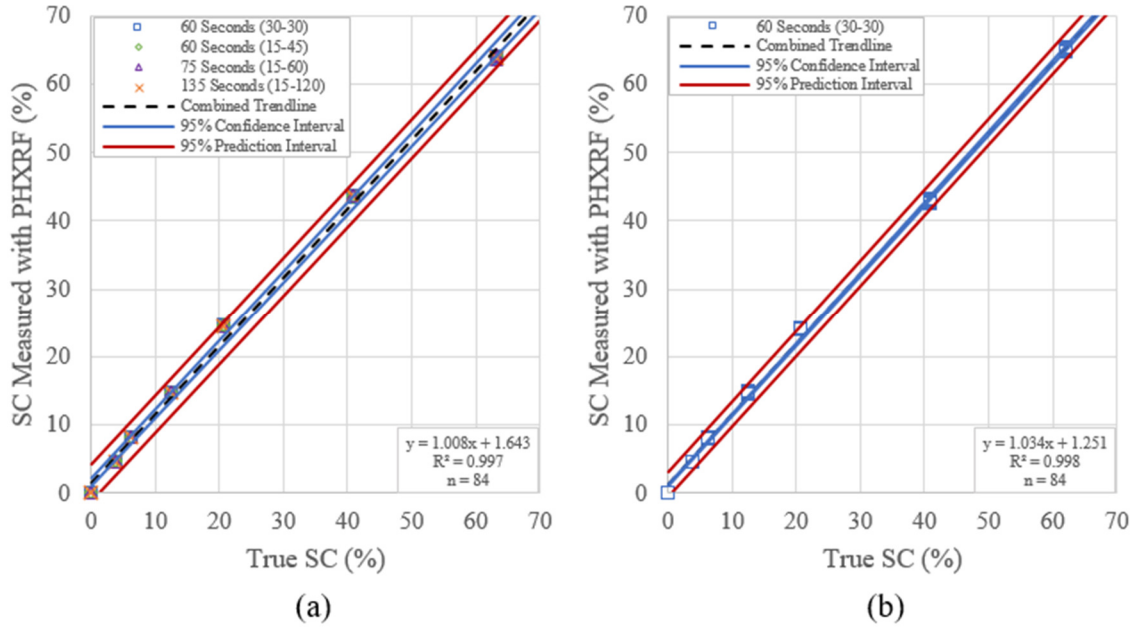


Figure 20: Effects of (a) Standard and (b) Quartering Scan Techniques on Precision and Accuracy of S1 Titan PHXRF Device for SGB Samples

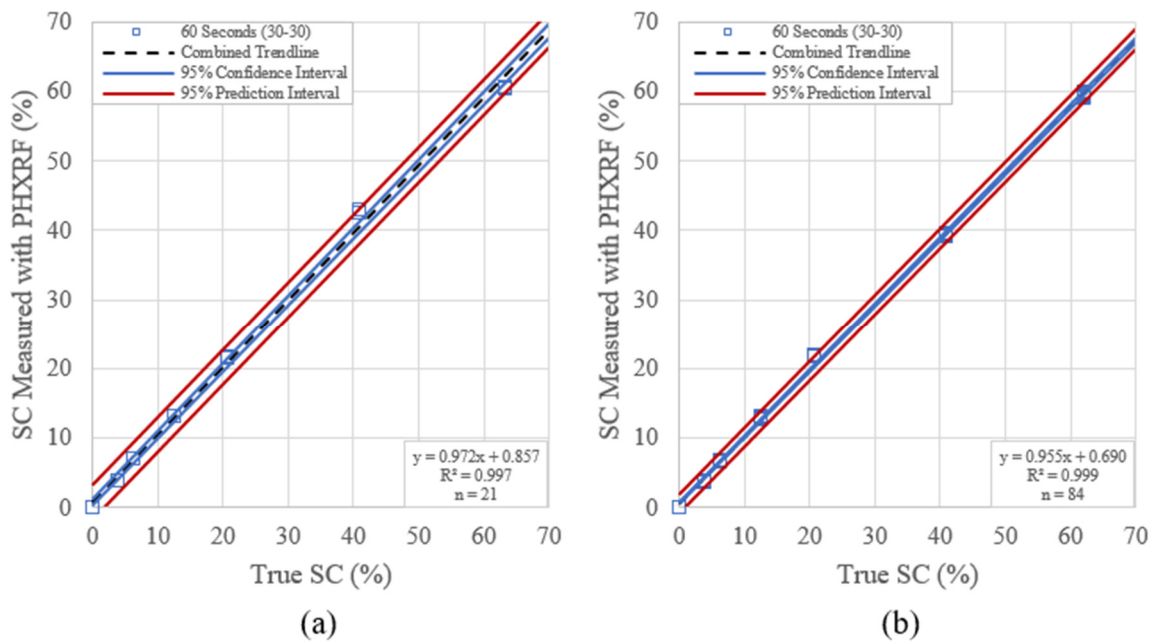


Figure 21: Effects of (a) Standard and (b) Quartering Scan Techniques on Precision and Accuracy of Niton XL3t PHXRF Device for SGB Samples.

4.2.2 Particle Size

Particle size plays a more prominent role in the accuracy of the PHXRF devices. Significant drops in RMSD are observed as samples are milled to smaller particle sizes. The relationship between precision and particles size, on the other hand, is minor according to the COV_{STDEV} .

As seen in Table 10, the relationship between precision and particle size is similar to that of precision and scan durations: insignificant. Once again, an example is the best way to demonstrate this point. If the mean value of a series of *SC* measurements is 21.844%, then scanning the passing No. 4 samples or the passing No. 200 samples would produce measurements of 21.844 ± 0.024 or 21.844 ± 0.091 , respectively, 95% of the time. Only the second decimal place of the measurements is affected, which is of minimal consequence as indicated by the near constant COV_{STDEV} . Conversely, accuracy is heavily influenced by particle size. The RMSD, or the deviation of the *SC* measurements from the true (commercial laboratory) *SC*, is decreased by 0.342% and 0.334% for the S1 Titan and Niton XL3t, respectively, when the particle size is reduced from passing the No. 4 sieve to passing the No. 200 sieve. The reduction in COV_{RMSD} , or variability of the measurements relative to the true *SC* value, confirm that milling samples to smaller particle diameters yield sizable benefits to PHXRF device accuracy.

Table 10: Effects of Particle Size on $STDEV$, COV_{STDEV} , $RMSD$,
and COV_{RMSD} for OHC Samples

	Particle Size (Passing)	n	$STDEV$. (%)	COV_{STDEV}	$RMSD$ (%)	COV_{RMSD}
S1 Titan	No. 4	280	0.035	0.001	1.234	0.082
	No. 40	280	0.025	0.001	0.892	0.062
	No. 100	280	0.024	0.001	0.915	0.077
	No. 200	240	0.036	0.001	0.905	0.056
Niton XL3t	No. 4	21	0.064	0.004	2.128	0.080
	No. 40	21	0.091	0.004	1.578	0.064
	No. 100	21	0.050	0.002	1.663	0.064
	No. 200	18	0.064	0.003	1.794	0.066

The results from the SGB samples agree with those of the OHC samples. These results can be seen in Table 11. Precision remains relatively unaffected while accuracy receives substantial benefits as sample particle diameter is reduced. The increase in accuracy is much more pronounced for the SGB samples, however. The RMSD of the SGB samples decrease by 1.251% for the S1 Titan and 0.723% for the Niton XL3t as particle size is reduced as opposed to 0.342% and 0.334% for the OHC samples. Though the magnitudes of increased accuracy vary between soils, there is unanimous agreement that milling samples to smaller particle sizes increases PHXRF device accuracy.

Table 11: Effects of Particle Size on $STDEV$, COV_{STDEV} , $RMSD$,
and COV_{RMSD} for SGB Samples

	Particle Size (Passing)	n	$STDEV$. (%)	COV_{STDEV}	$RMSD$ (%)	COV_{RMSD}
S1 Titan	No. 4	84	0.032	0.001	3.560	0.246
	No. 40	84	0.039	0.001	2.601	0.190
	No. 100	84	0.045	0.002	2.323	0.156
	No. 200	84	0.020	0.001	2.309	0.159
Niton XL3t	No. 4	21	0.155	0.006	1.607	0.089
	No. 40	21	0.075	0.004	1.293	0.057
	No. 100	21	0.135	0.006	0.884	0.055
	No. 200	21	0.105	0.006	0.984	0.056

Linear regression analyses were used to examine the statistical significance of the effects of various particle sizes on precision and accuracy of PHXRF devices. The results of the OHC and SGB measurements for the S1 Titan are presented in Figure 22 and Figure 24, respectively; for the Niton XL3t, Figure 23 and Figure 25. Regression line (a) is produced from all passing No. 4 scans, (b) is produced from all passing No. 40 scans, etc. In most cases as particle size decreases, the bands of both the 95% confidence interval and the 95% prediction interval tend to converge on the combined trendline and the combined trendline moves closer to the $y = x$ line. This is caused by a decrease in the spread of each set of measurements, which indicates higher accuracy. This trend is observed in the OHC samples scanned by the S1 Titan and more pronounced in the SGB samples scanned by both devices. Furthermore, these changes are substantial enough to place the combined trendline for (a) outside of the 95% confidence bands of (b), place the combined trendline for (b) outside of the 95% confidence

band of (c), etc. This verifies that particle size is a variable of statistical significance regarding PHXRF measurements.

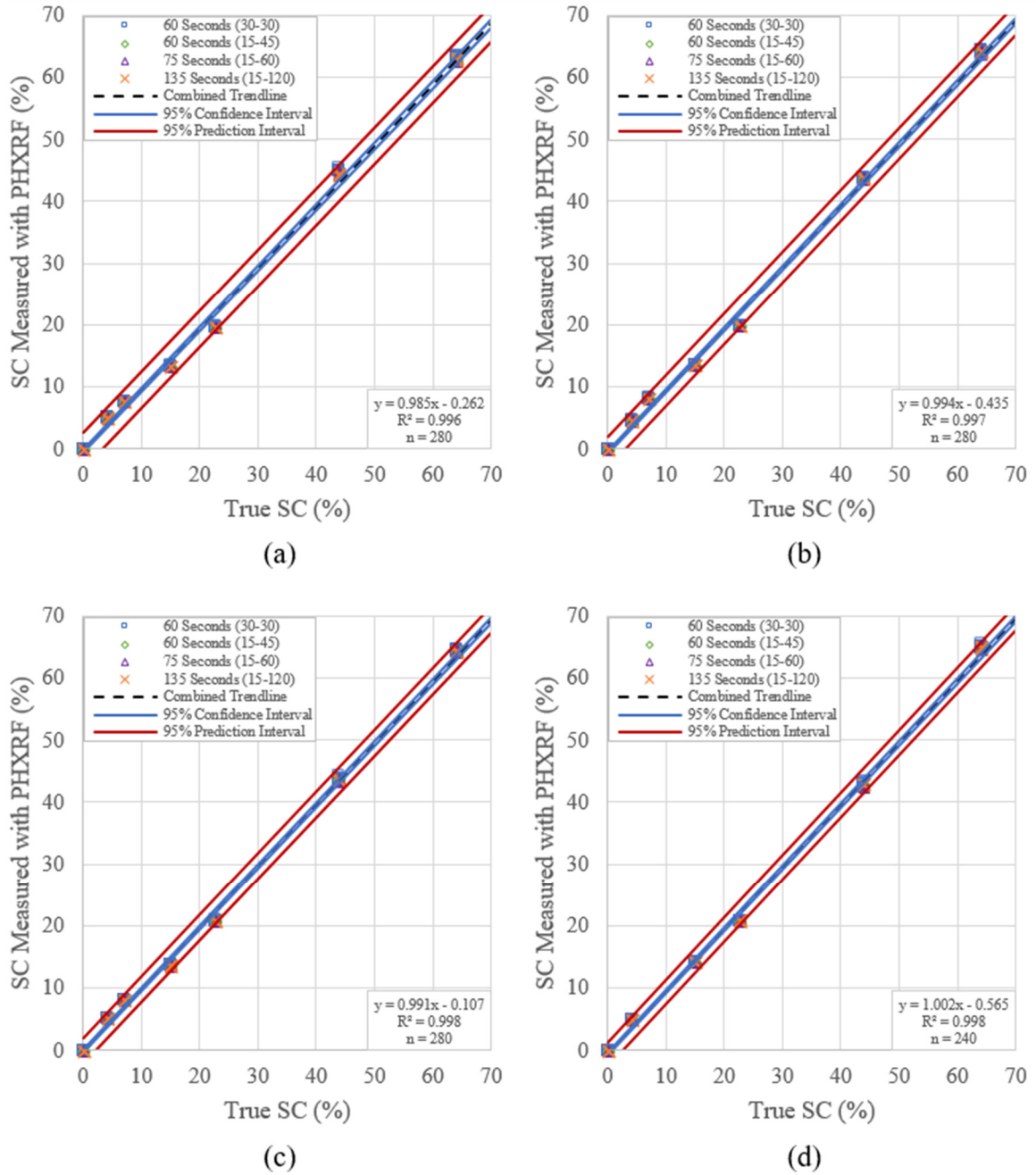


Figure 22: Effects of Various Particle Sizes on Precision and Accuracy of S1 Titan PHXRF Device for (a) Passing No. 4, (b) Passing No. 40, (c) Passing No. 100, and (d) Passing No. 200 particle size OHC samples.

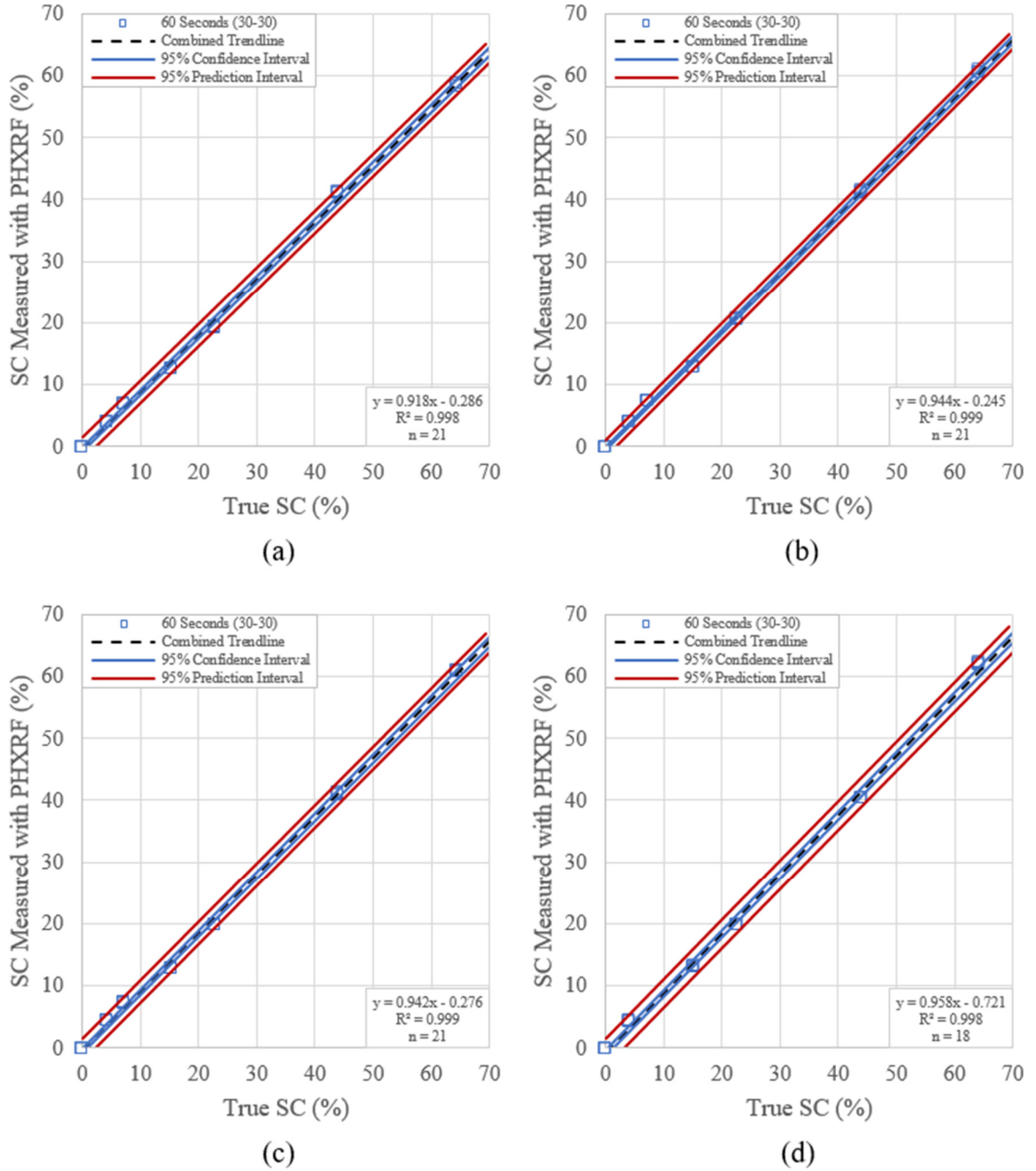


Figure 23: Effects of Various Particle Sizes on Precision and Accuracy of Niton XL3t PHXRF Device for (a) Passing No. 4, (b) Passing No. 40, (c) Passing No. 100, and (d) Passing No. 200 particle size OHC samples.

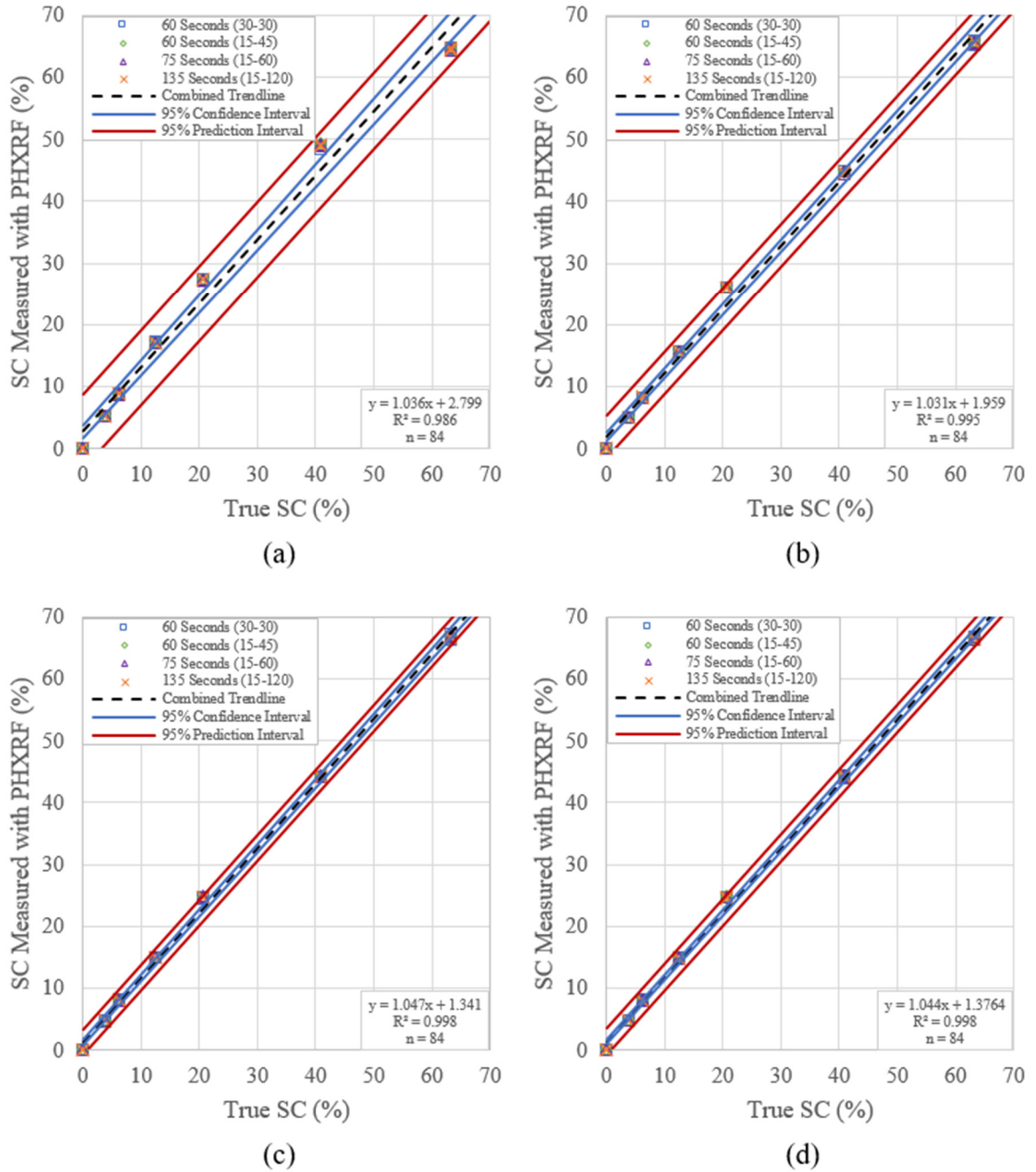


Figure 24: Effects of Various Particle Sizes on Precision and Accuracy of S1 Titan PHXRF Device for (a) Passing No. 4, (b) Passing No. 40, (c) Passing No. 100, and (d) Passing No. 200 particle size SGB samples.

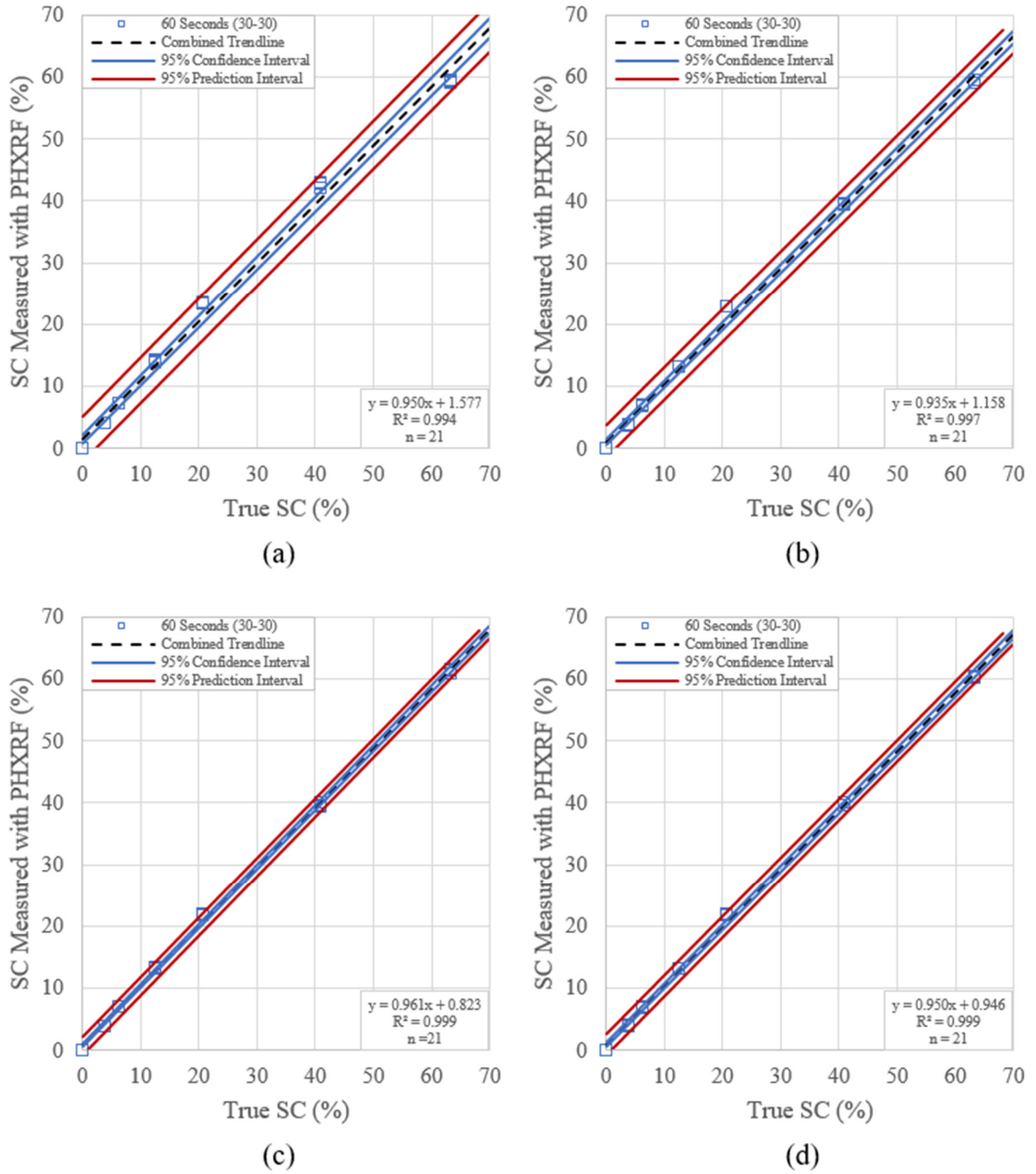


Figure 25: Effects of Various Particle Sizes on Precision and Accuracy of Niton XL3t PHXRF Device for (a) Passing No. 4, (b) Passing No. 40, (c) Passing No. 100, and (d) Passing No. 200 particle size SGB samples.

Theoretically, the most accurate samples for all cases should have the smallest particle size (i.e. passing No. 200). Interestingly, this principle was only observed in the SGB samples scanned by the S1 Titan. A possible explanation for this deviation from theory could be the presence of oxygen during the scans. XRF laboratories and many benchtop units often flush the sample chamber with helium to improve device sensitivity for light elements such as calcium. PHXRF are rarely equipped with such an option. On average, however, the samples with particle sizes that pass the No. 100 sieve have the smallest RMSD, which is 1.446%, and samples with the smallest particle size have the smallest COV_{RMSD} , which is 0.084. Average RMSD and COV_{RMSD} for all samples and both devices can be seen in Table 12.

Table 12: Average RMSD and COV_{RMSD} for All Samples and Both PHXRF Devices

<i>Particle Size (Passing)</i>	<i>n</i>	<i>Avg. RMSD (%)</i>	<i>Avg. COV_{RMSD}</i>
<i>No. 4</i>	<i>406</i>	<i>2.132</i>	<i>0.124</i>
<i>No. 40</i>	<i>406</i>	<i>1.591</i>	<i>0.093</i>
<i>No. 100</i>	<i>406</i>	<i>1.446</i>	<i>0.088</i>
<i>No. 200</i>	<i>363</i>	<i>1.498</i>	<i>0.084</i>

In terms of field feasibility, milling samples to pass the No. 100 and No. 200 sieves is a laborious and time consuming endeavor. This degree of preparation rigor is not practical on site. It may be more conducive to limit milling to passing the No. 40 sieve. As seen in Figure 26, benefits to PHXRF accuracy, both in terms of RMSD and COV_{RMSD} , begin to level off once a sample particle size is reduced

passed the No. 40 sieve. For this reason and for the sake of time and cost, it was decided that all field samples would be milled to pass the No. 40 sieve.

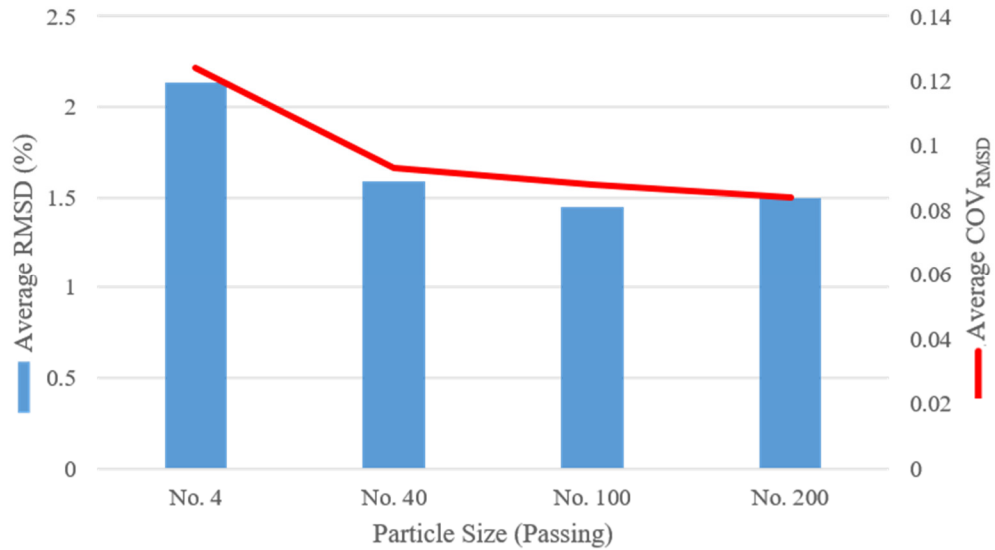


Figure 26: Average RMSD and Average COV_{RMSD} as a Function of Particle Size

4.2.3 Sample Type

The sample types used in this research were pressed pellets and powder samples. The role that sample type plays in the precision and accuracy of PHXRF SC measurements is inconclusive. PHXRF precision appears to be independent of sample type; meanwhile, equitable gains in accuracy are observed when a sample is prepared into a pellet for the OHC soil type, but the opposite is observed in the SGB ones.

As seen in Table 13, precision varies randomly. Ultimately, this is of little concern, as is indicated by the nearly unaffected COV_{STDEV} for both devices. This suggests that sample type does not influence the precision of PHXRF SC

measurements. The same cannot be said for accuracy. Deviations in PHXRF *SC* measurements from the true *SC* of the OHC samples are greatly increased when using powder samples. The deviations for the S1 Titan and Niton XL3t increase by as much as 1.248% and 1.006%, respectively. The significance of these changes is verified by the large changes in COV_{RMSD} for both devices. The scatter of the PHXRF *SC* measurements relative to the true *SC* jumps from 0.056 to 0.133 for the S1 Titan and 0.066 to 0.096 for the Niton XL3t. The results of both devices suggest that pressed pellets produce significantly more accurate results than their powder sample counterparts.

Table 13: Effects of Sample Type on STDEV, COV_{STDEV}, RMSD, and COV_{RMSD} for OHC Samples

	<i>Sample Type</i>	<i>n</i>	<i>STDEV (%)</i>	<i>COV_{STDEV}</i>	<i>RMSD (%)</i>	<i>COV_{RMSD}</i>
<i>S1 Titan</i>	<i>Pellet</i>	240	0.036	0.001	0.905	0.056
	<i>Powder</i>	240	0.029	0.001	2.153	0.133
<i>Niton XL3t</i>	<i>Pellet</i>	18	0.064	0.003	1.794	0.066
	<i>Powder</i>	18	0.099	0.005	2.800	0.096

The results from the SGB analysis sharply contrasts those of the OHC samples in terms of accuracy. They agree, however, regarding precision. These results can be seen in Table 14. The negligible changes in COV_{STDEV} for both instruments once again confirm that sample type plays little to no role in the

precision of the PHXRF instruments. The conflict in results occurs in the RMSD and COV_{RMSD} for both instruments. For the SGB samples, accuracy is improved when using powder samples, as is indicated by the decrease in RMSD and COV_{RMSD} . The results of both devices on the SGB samples suggest that powder samples produce more accurate results than their pressed pellet counterparts, again conflicting with the OHC results and the literature.

Table 14: Effects of Sample Type on STDEV, COV_{STDEV} , RMSD, and COV_{RMSD} for SGB Samples

	<i>Sample Type</i>	<i>n</i>	<i>STDEV (%)</i>	<i>COV_{STDEV}</i>	<i>RMSD (%)</i>	<i>COV_{RMSD}</i>
<i>S1 Titan</i>	<i>Pellet</i>	280	0.020	0.001	2.309	0.159
	<i>Powder</i>	280	0.035	0.003	1.808	0.145
<i>Niton XL3t</i>	<i>Pellet</i>	21	0.105	0.006	0.984	0.056
	<i>Powder</i>	21	0.068	0.004	0.980	0.051

Regardless, the question of statistical significance still remains. Are the accuracy benefits observed in the OHC results significant enough to prove that pressed pellets are the better option? On the other hand, are the accuracy detriments observed in the SGB results significant enough to prove that powder samples are the better option? Interestingly, linear regression analyses verify both. The results of the OHC and SGB measurements for the S1 Titan are illustrated in Figure 27 and Figure 29, respectively; for the Niton XL3t, Figure 28 and Figure

30. Figure 27 and Figure 28 support the case that pressed pellets are the better option. The variations in slopes and y-intercepts are large enough to place the combined trendlines outside of the 95% confidence intervals of the corresponding graphs. This statistically verifies that pressed pellets produce more accurate PHXRF *SC* measurements. Figure 29, however, verifies the contrary (i.e. powder samples produce more accurate PHXRF *SC* measurements). Still, Figure 30 verifies no statistically significant benefit or detriment to the accuracy of PHXRF *SC* measurements caused by sample type.

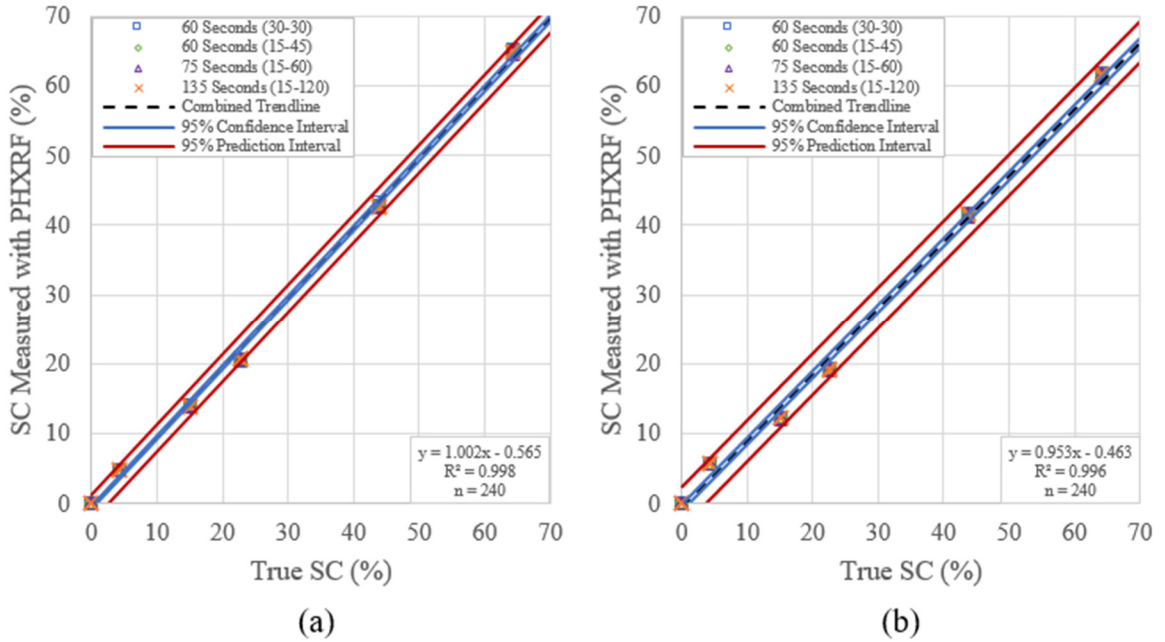


Figure 27: Effects of (a) Pressed Pellet and (b) Powder Sample Types on Precision and Accuracy of S1 Titan PHXRF Device for OHC Samples.

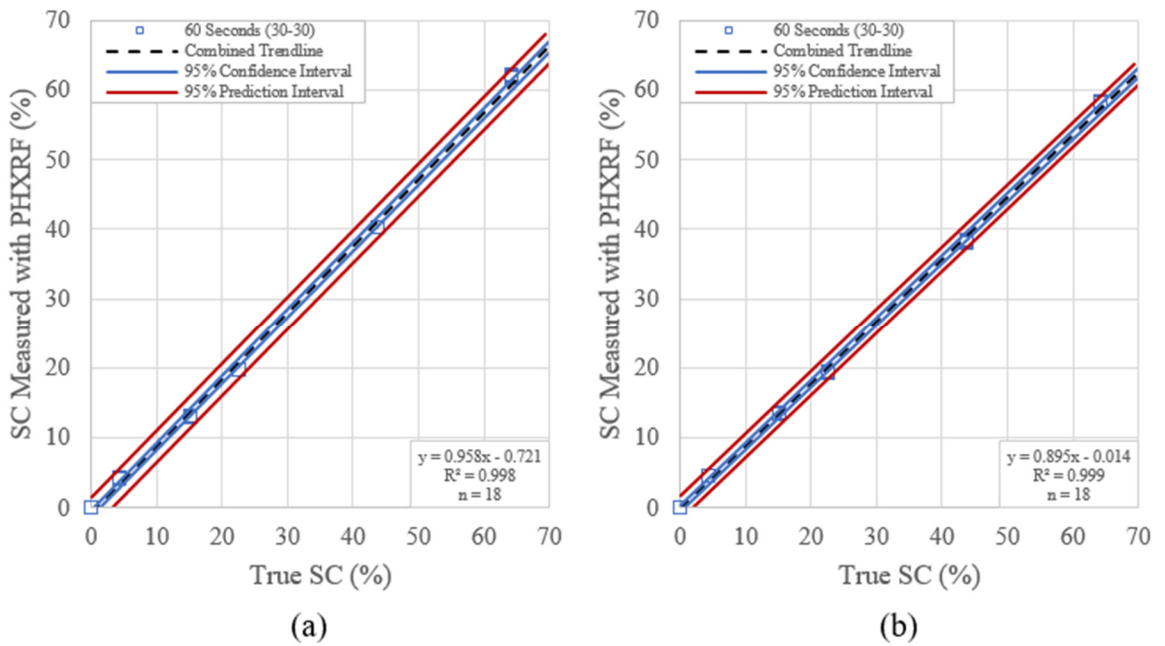


Figure 28: Effects of (a) Pressed Pellet and (b) Powder Sample Types on Precision and Accuracy of Niton XL3t PHXRF Device for OHC Samples.

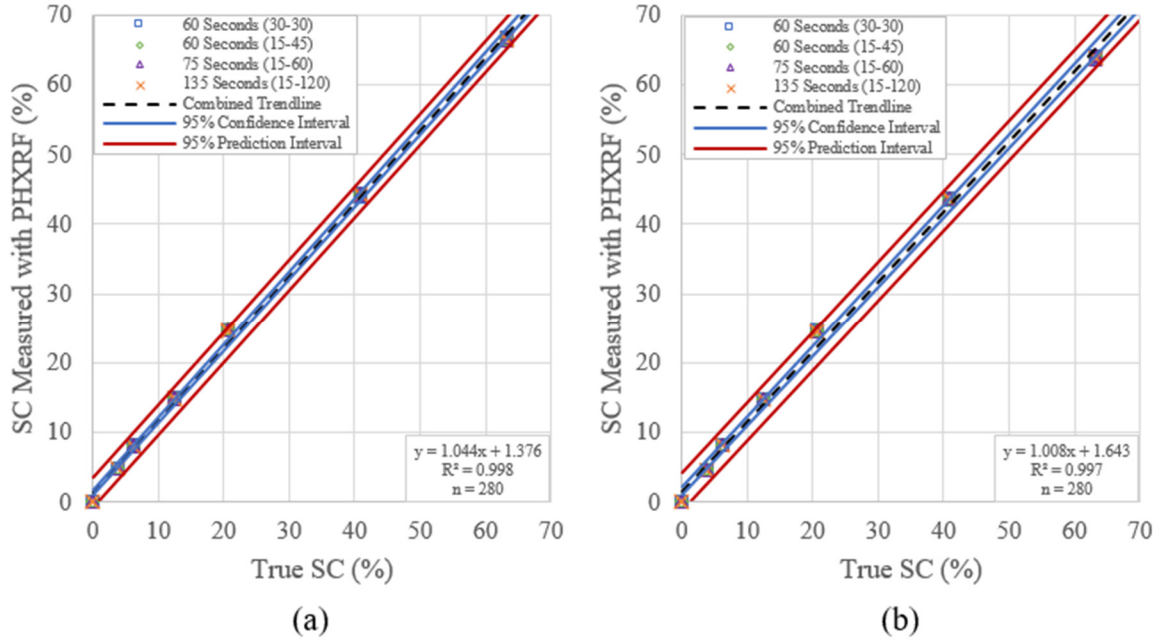


Figure 29: Effects of (a) Pressed Pellet and (b) Powder Sample Types on Precision and Accuracy of S1 Titan PHXRF Device for SGB Samples.

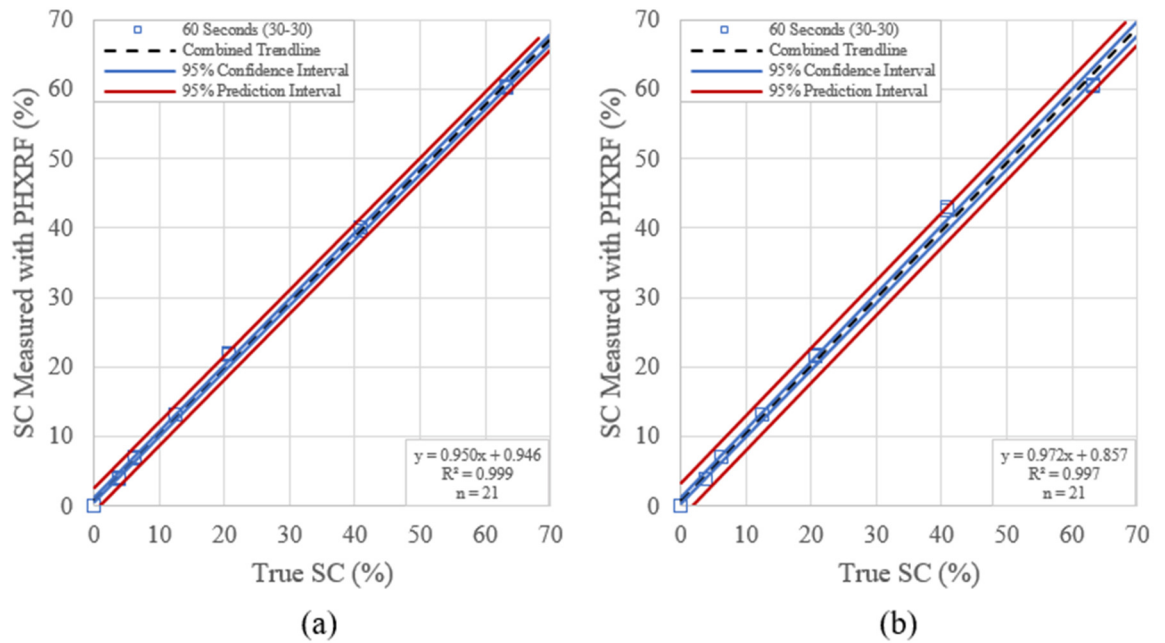


Figure 30: Effects of (a) Pressed Pellet and (b) Powder Sample Types on Precision and Accuracy of Niton XL3t PHXRF Device for SGB Samples.

Figure 31 further illustrates the inconsistencies in the sample type results. As can be seen in the OHC chart (left), pressed pellets clearly reduce RMSD of the PHXRF SC measurements, thus increasing accuracy. Nonetheless, the SGB chart (right) clearly shows that powder samples reduce RMSD for the S1 Titan SC measurements and make no difference in RMSD for the Niton XL3t. Ultimately, it was decided that the results regarding sample type are inconclusive. Accordingly, all field samples would be processed into powder samples because they require significantly less time and labor to prepare compared to their pressed pellet counterparts.

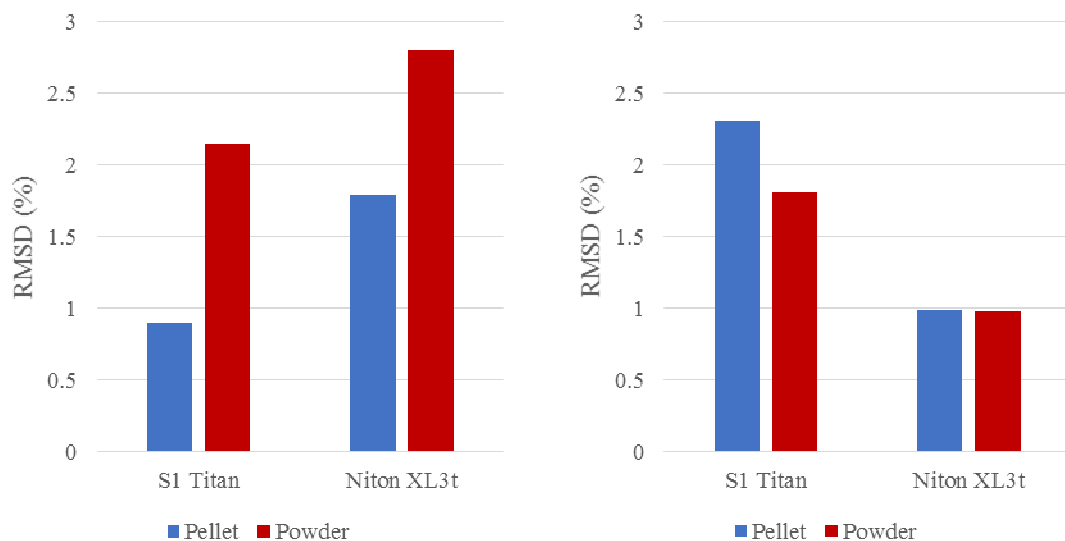


Figure 31: RMSD for OHC (Left) and SGB (Right) Pellet and Powder Samples

4.2.5 PHXRF Device Comparison

The direct comparison between the S1 Titan and Niton XL3t show that neither device is conclusively better than the other at detecting *SC* in subgrade soils. The S1 Titan proves to have more precise measurements; however, the accuracy of each device appears to be a function of soil type. For example, the S1 Titan is much more accurate than the Niton XL3t at detecting *SC* in the OHC samples, while the Niton XL3t is considerably more accurate at detecting *SC* in the SGB samples.

As seen in Table 15, the S1 Titan produces slightly more precise measurements than the Niton XL3t for both OHC and SGB soil samples. Taking measurements with the S1 Titan reduces the $STDEV$ by 0.013% and 0.025% in OHC and SGB samples, respectively. This is of very little consequence, however, as is indicated by the trivial differences in the COV_{STDEV} . Accuracy of each device seems to depend on the soil type, which may be caused by differences in factory soil calibrations. Deviations from the true *SC* of the OHC samples, as measured by the commercial laboratory using the whole rock method, are reduced by .783% when using the S1 Titan, whereas for the SGB samples, it is reduced by 1.365% when using the Niton XL3t. Interestingly, the Niton XL3t has the lowest variability in relation to the true *SC* for both soils. This suggests that the Niton XL3t may be the better choice for determining *SC* in subgrade soils than the S1 Titan. On the other hand, the differences in accuracy of the two devices may likely be the result of different factory soil calibrations. The calibration for the S1 Titan

may be more appropriate for Kaolinite-based clay, whereas the Niton XL3t calibration may be more suited for Montmorillonite-based clay.

Table 15: Direct Comparison of S1 Titan and Niton XL3t Measurements

	PHXRF Device	<i>n</i>	STDEV (%)	COV _{STDEV}	RMSD (%)	COV _{RMSD}
OHC	S1 Titan	99	0.060	0.002	1.191	0.082
	Niton XL3t	99	0.073	0.004	1.974	0.074
SGB	S1 Titan	105	0.082	0.003	2.515	0.177
	Niton XL3t	105	0.107	0.005	1.150	0.060

Linear regressions for OHC and SGB samples are illustrated in Figure 32. The figures clearly display that the S1 Titans scans of the OHC samples fall closer to the one to one line than those of the Niton XL3t, indicating that, in this study, the S1 Titan was more accurate. Conversely, the Niton XL3t scans of the SGB samples fall much closer to the one to one line than those of the S1 Titan. This agrees with the findings in the previous paragraph. Accordingly, both devices may be appropriate for determining *SC* in subgrade soils as long as the soil being tested is agrees with the calibration of the device. In an unknown soil setting, however, the Niton XL3t may be the more appropriate choice.

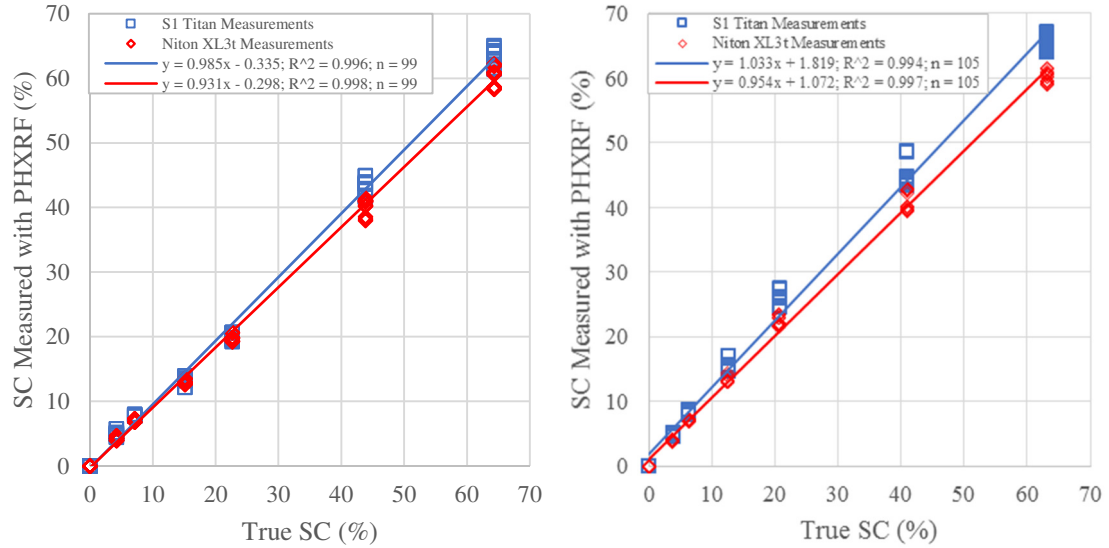


Figure 32: Direct Comparison of S1 Titan and Niton XL3t

Measurements for OHC Samples (Left) and SGB Samples (Right)

4.3 PHXRF Field Testing

The results from in situ accuracy, ex situ accuracy, and homogeneity tests are presented in the following paragraphs. All SC measurements for the field studies were taken with the Niton XL3t only.

4.3.1 In Situ PHXRF Measurement Accuracy

In situ PHXRF measurements differ greatly from measurements made by a commercial laboratory. In fact, there appears to be no relationship between the two. The in situ PHXRF measurements were simply surface shots of the soil, with no soil preparation except a leveling and tamping of the ground, while the commercial laboratory processed each sample by melting them into fluxed discs. Additionally, precision and accuracy varies unpredictably between

measurements, which indicate that in situ PHXRF measurements, with no sample preparation, are not appropriate for determining *SC* in subgrade soils.

As seen in Table 16, in situ measurements with the Niton XL3t at random grid locations throughout Site 2 produce random results. STDEV varies from 0.534% to 4.139% despite using a standard scanning technique. The COV_{STDEV} for the Niton XL3t measurements are also sporadic and ranges from 0.013 to 0.099. Accuracy of the measurements is very poor as well. The RMSD range from 19.468 to 32.444, which is far outside of allowable limits. Additionally, the COV_{RMSD} range from 0.925 to 2.435, which indicates significant errors in these measurements. Plainly, the device performed poorly when the soil was not prepared adequately. This could be for a number of reasons, including particle size effects, surface roughness, soil being blown into the scanning window via wind, the presence of oxygen, and the presence of moisture, to name a few.

Table 16: Precision and Accuracy of Niton XL3t In Situ Measurements at Random Grid Locations throughout Site 2

	<i>Location</i>	<i>n</i>	<i>STDEV (%)</i>	COV_{STDEV}	<i>RMSD (%)</i>	COV_{RMSD}
<i>Niton XL3t</i>	4	3	0.534	0.013	19.468	0.953
	16	3	4.139	0.099	20.207	0.925
	27	3	1.857	0.041	32.444	2.435

The linear regression analysis confirms the poor performance of the PHXRF during in situ testing. The results are illustrated in Figure 33. The large

areas that lie between the 95% confidence interval and 95% prediction interval signify poor precision of the PHXRF measurements, while the deviation from the $y = x$ line proves poor device accuracy in situ. Additionally, the low coefficient of determination, R^2 , suggests that the combined trendline poorly fits the data points. This implies that even when the PHXRF measurements are mathematically corrected using the equation of the combined trendline, large errors will still be present. For these reasons, in situ measurements are not appropriate for determining SC in subgrade soils.

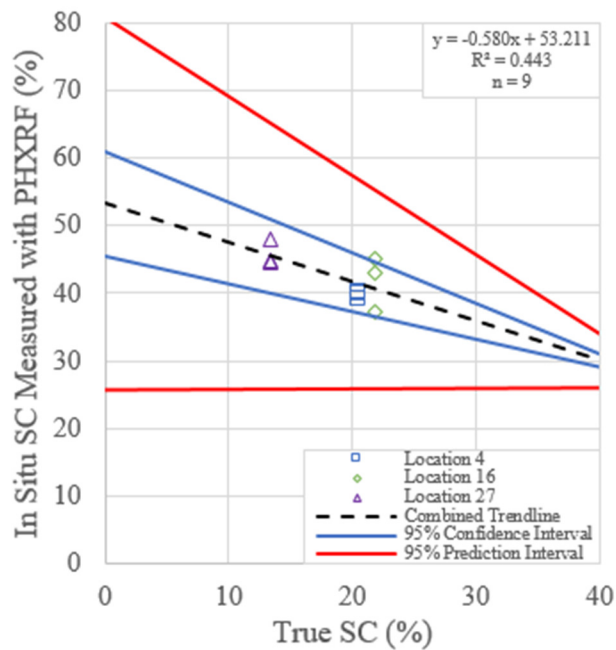


Figure 33: Linear Regression of Site 2 In Situ Measurements with the Niton XL3t PHXRF

4.3.2 Ex Situ PHXRF Measurement Accuracy

Ex situ PHXRF measurements, which were field sampled soils brought back to the laboratory, processed over a number 40 sieve, and placed in a sample cup, are much more consistent with those made by a commercial laboratory. Strong correlations can be made between the two. Additionally, precision and accuracy are much more stable between measurements, which seem to indicate systematic errors that can possibly be corrected mathematically. For these reasons, ex situ PHXRF measurements may be appropriate for determining *SC* in subgrade soils.

As seen in Table 17, ex situ measurements with the Niton XL3t at random locations throughout Site 2 produce fairly consistent results. STDEV vary from 0.345% to 0.579% despite using a quartering scan technique. The COV_{STDEV} for the Niton XL3t measurements are also relatively regular, ranging only from 0.021 to 0.030. Accuracy of the measurements is very poor. The RMSD range from 8.330 to 11.574 and the COV_{RMSD} range from 0.812 to 1.025, which are both outside of limitations and indicate significant errors in these measurements. Despite this, these errors are much more consistent than those observed in the in situ PHXRF measurements. For this reason, mathematical corrections may be useful for ex situ PHXRF measurements.

Table 17: Precision and Accuracy of Niton XL3t Ex Situ Measurements at Random Locations throughout Site 2

	<i>Location</i>	<i>n</i>	<i>STDEV (%)</i>	<i>COV_{STDEV}</i>	<i>RMSD (%)</i>	<i>COV_{RMSD}</i>
<i>Niton XL3t</i>	4	12	0.424	0.021	11.574	0.872
	16	12	0.579	0.030	9.551	1.025
	27	12	0.345	0.026	8.330	0.812

The linear regression analysis confirms the consistency of the errors in the ex situ PHXRF measurements. The results are illustrated in Figure 34. The tightness of both the 95% confidence intervals and 95% prediction intervals signify strong precision of the PHXRF measurements. The deviation from the one to one line shows poor device accuracy in ex situ conditions; however, the combined trendline fits the data points remarkably well with an R^2 equal to 0.925. This implies that the PHXRF measurements are mathematically corrected using the equation of the combined trendline, to obtain accurate results. For these reasons, ex situ measurements may be appropriate for determining *SC* in subgrade soils.

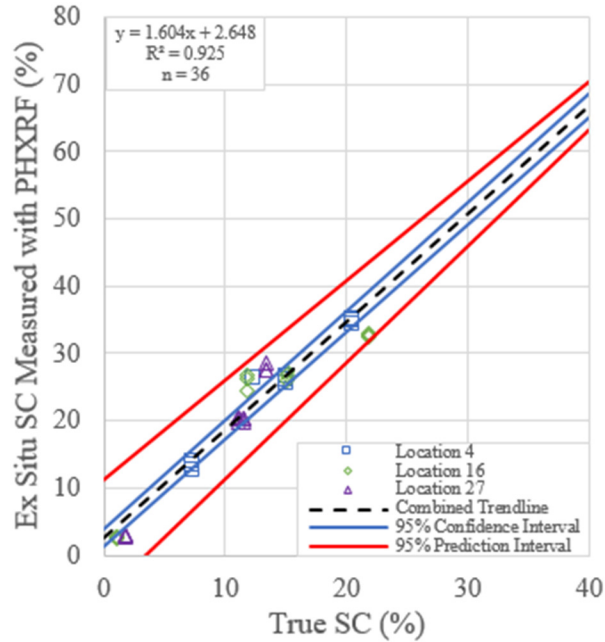


Figure 34: Linear Regression of Site 2 Ex Situ Measurements with the Niton XL3t PHXRF

4.3.3 Spatial Stabilizer Homogeneity

Spatial heterogeneity was present in each stabilization site that was investigated. Large variations in *SC* were observed throughout each site, which may lead to problematic conditions, such as pavement deformation, in the future.

4.3.3.1 Site 1

The idealized and calculated (using the equation found in Figure 34) spatial distributions of *SC* for Site 1 are illustrated in Figure 35. The corrected ex situ PHXRF measurements in the top nine inches of Site 1 are found to have an average *SC* of 15.3%. This result is encouraging considering the design CKD *SC* is 15% for this site. Therefore, an error of

only 0.3% is detected. In addition to *SC* accuracy, observations of spatial distribution of *SC* can be made. Considerable relative disparities in *SC* are present throughout the area of Site 1. For example, a large amount of stabilizer seems to have been unproportionally spread to the northwest corner of the site. In the top 3 inches of the site, corrected stabilizer contents between lengths 20 ft and 50 ft and widths 0 ft and 2.5 ft range from 17.9% to 22.6%; meanwhile between lengths 5 ft and 15 ft, corrected *SC* falls between 9.6% and 14.2%. Additionally in the 3 to 6 in layer, corrected *SC*s between lengths 25 ft and 30 ft and widths 0 ft and 2.5 ft rise as high as 24.7%, which sharply contrasts 7.5% while occurs at lengths 0 ft to 5 ft and widths 7.5 ft to 10 ft. These vast differences in *SC* suggests that improved spreading and mixing measures may need to be taken to produce a more homogenous site.

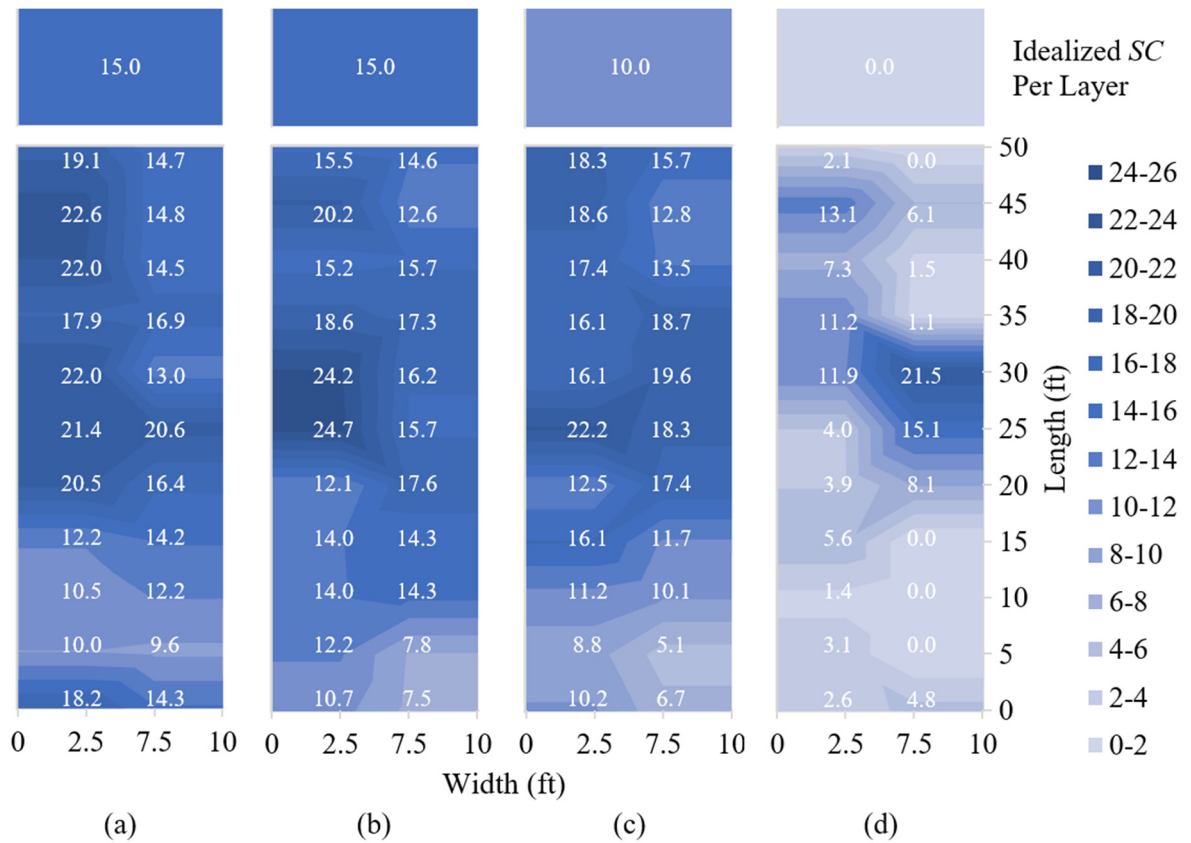


Figure 35: Idealized and Corrected Spatial Stabilizer Distribution for Site 1 at Depths of (a) 0 - 3, (b) 3 - 6, (c) 6 - 9, and (d) 9 - 12 Inches

Another issue observed with Site 1 is a portion of the layer below a depth of 8 inches was stabilized. This area is located between lengths 25 ft. and 35 ft. and widths 7.5 ft. and 10 ft. Corrected SC in this area is measured to be 21.5%. All soil below 8 inches should remain undisturbed and not be stabilized. This site is unique for the fact that it had been stabilized 30 years prior to the current construction. Elevated levels of CaO compared to other test sites were detected in the “raw” soil before current treatment, however nowhere near the levels that would constitute

a *SC* of 20+%. The degree of variance in *SC* from 9 to 12 inches may more likely have been caused by faulty mixing depth and/or leaching of stabilizer into the soil below the stabilized area.

4.3.3.2 Site 2

The idealized and corrected spatial distribution of *SC* for Site 2 are illustrated in Figure 36. The corrected ex situ PHXRF measurements in the top nine inches of Site 2 are found to have an average *SC* of 12.6%. This result is slightly low compared to the design fly ash *SC*, which is 16%. An error of 3.4% is detected in this site. Spatial analysis shows that significant disparities in *SC* are observed throughout the site. For example, a large amount of stabilizer seems to have been unproportionally spread to the west side of the site. In the top 3 inches, corrected stabilizer contents between lengths 0 ft and 10 ft and width 0 ft range from 20.1% to 23.4%; meanwhile between lengths 45 ft and 50 ft, corrected *SC* falls between 7.4% and 11.2%. Additionally in the 3 to 6 and 6 to 9 layers, there is a spot at length 45 ft and width 10 ft that has a measured *SC* of zero. The findings of Site 2 agree with those of Site 1 (i.e. improved spreading and mixing measures may need to be taken to produce a more homogenous site).

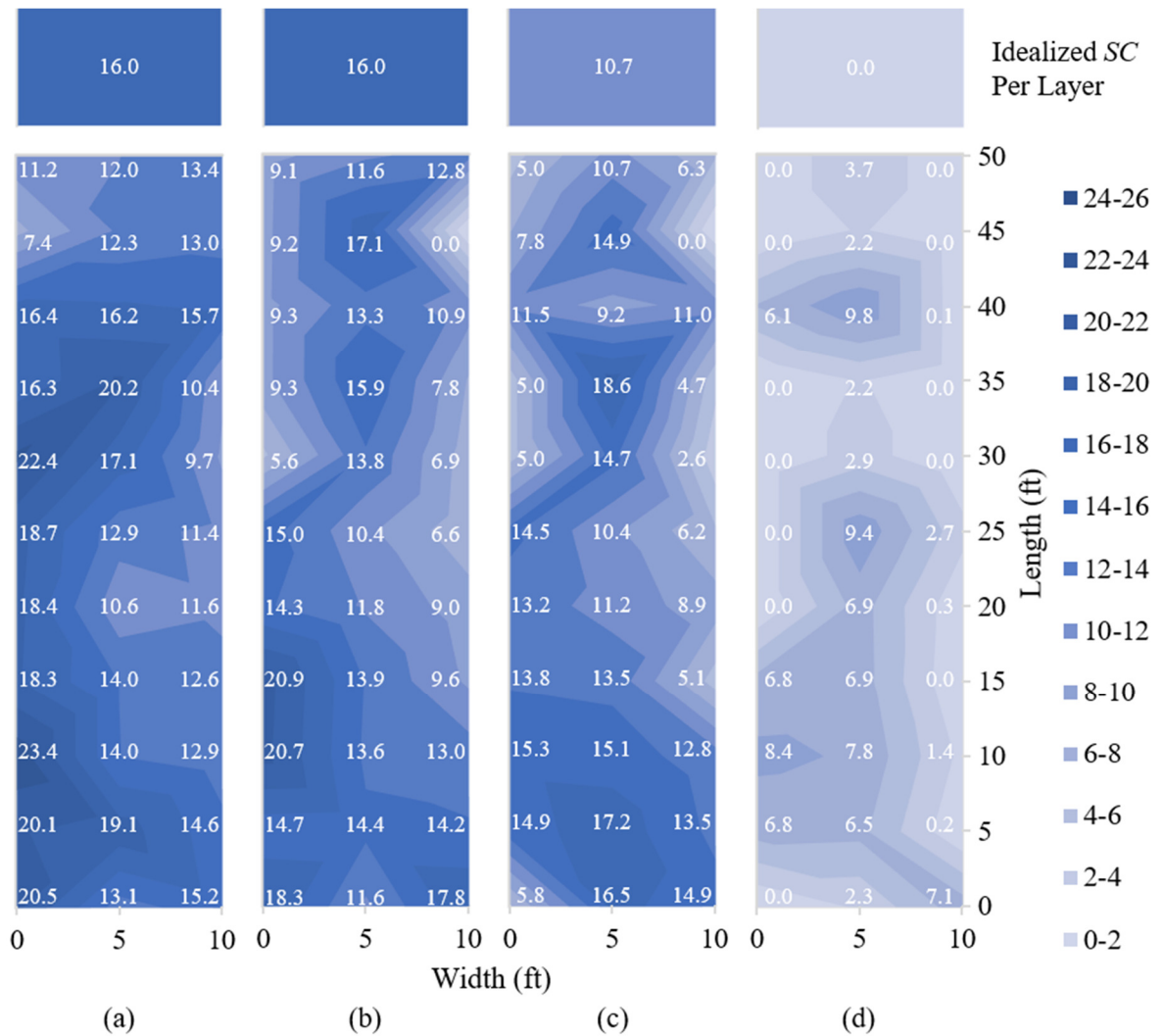


Figure 36: Idealized and Corrected Spatial Stabilizer Distribution for Site 2 at Depths of (a) 0 - 3, (b) 3 - 6, (c) 6 - 9, and (d) 9 - 12 Inches

4.3.3.3 Site 3

The idealized and corrected spatial distribution of SC for Site 3 is illustrated in Figure 37. The corrected ex situ PHXRF measurements found the top nine inches of Site 3 to have an average SC of 10.8%. This result is encouraging considering the design portland cement SC is 10%

for this site. Therefore, an error of only 0.8% is detected. Similarly to Sites 1 and 2, however, relative disparities in *SC* are observed throughout Site 3. Stabilizer seems to have been unproportionally spread to the east side of this site. In the top 3 inches of the site, corrected stabilizer contents between lengths 0 ft and 10 ft and width 10 ft range from 13.5% to 17.1%; meanwhile between lengths 0 ft and 10 ft and width 0 ft, corrected *SC* falls between 7.4% and 8.5%. Similar trends are observed throughout the depth of the site. This agrees with the findings of Site 1 and 2 that improved spreading and mixing measures may be needed to combat the variability throughout the site.

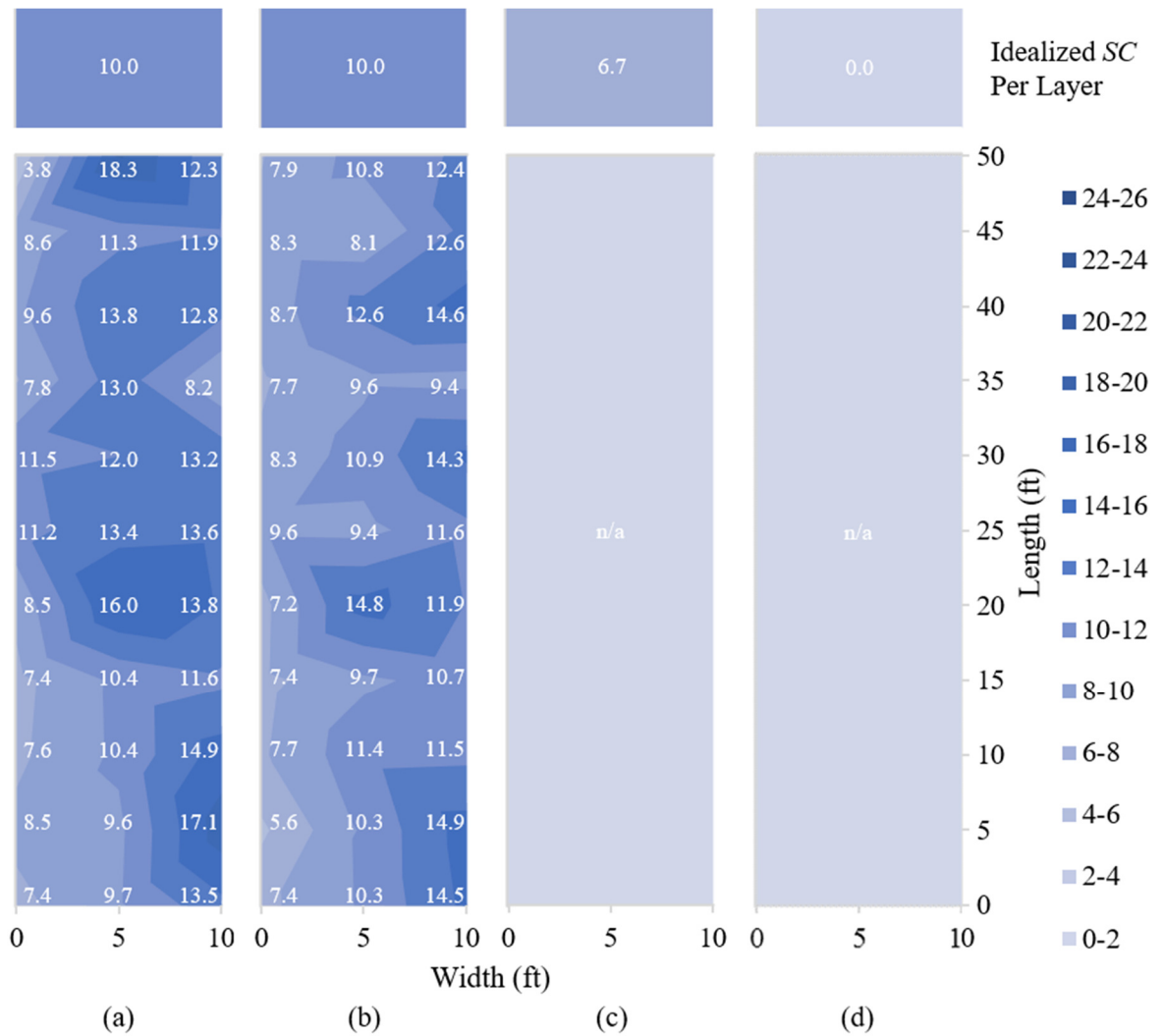


Figure 37: Idealized and Corrected Spatial Stabilizer Distribution for Site 3 at Depths of (a) 0 - 3, (b) 3 - 6, (c) 6 - 9, and (d) 9 - 12 Inches

The average SCs measured in the design volume of the sites with PHXRF spectrometry are often within $\pm 1\%$ of the design SCs, as seen in Table 18. This degree of accuracy, coupled with the convenience of portability of PHXRF devices, shows great promise regarding field deployment feasibility. PHXRF spectrometry is a very helpful

and efficient way of gathering data and can be a very useful tool for future construction site inspectors and forensic investigators.

Table 18: Average Ex Situ Stabilizer Content Measurements and Design Stabilizer Contents for Top Nine Inches of All Sites

	<i>Site Number</i>	<i>n</i>	<i>Measured SC (%)</i>	<i>Design SC (%)</i>
<i>Niton XL3t</i>	<i>1</i>	<i>198</i>	<i>15.3</i>	<i>15.0</i>
	<i>2</i>	<i>297</i>	<i>12.6</i>	<i>16.0</i>
	<i>3</i>	<i>198</i>	<i>10.8</i>	<i>10.0</i>

4.3.4 Depth Stabilizer Homogeneity

Depth heterogeneity is observed in all three sites. Analysis indicates that as depth increases, SC decreases. This trend can be seen in Figure 38. The degree of this decrease varies between sites. Ideally, SC measurements would stay constant to a depth of eight inches and then drop to zero percent below. While SC does decrease significantly below eight inches, there is still a large amount of stabilizer present at this depth. This conflicts with design specifications.

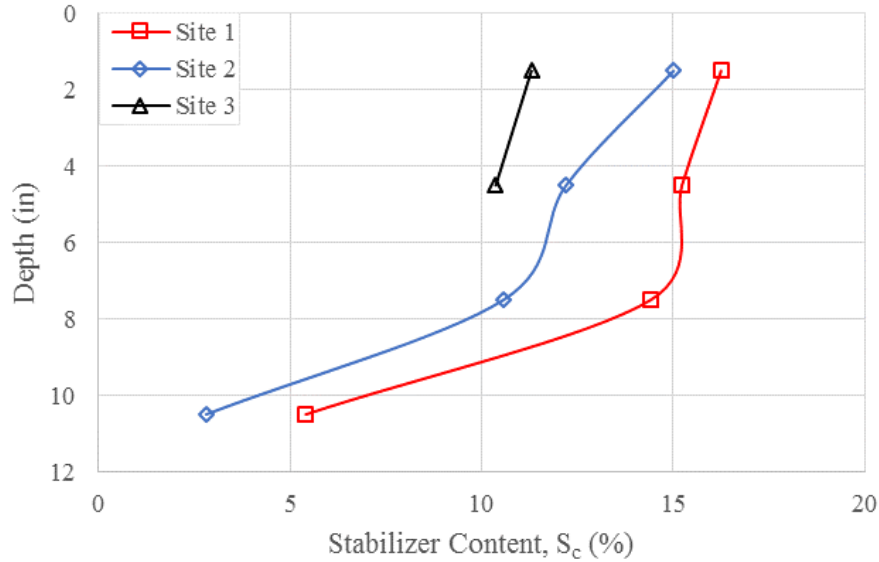


Figure 38: Depth Heterogeneity for All Sites

4.3.4.1 Site 1

The idealized depth distribution of SC and corrected ex situ PHXRF measurements with depth for Site 1 are illustrated in Figure 39. As seen in both figures, SC decreases below a depth of 8 inches. For depths 0 to 3, 3 to 6, 6 to 9, and 9 to 12 in, the corrected SC s on average are measured as 16.2%, 15.2%, 14.4% and 5.4%, respectively. These measured SC s are very close to the design CKD SC of 15%. The depth analysis agrees with the spatial analysis in that a disproportion of stabilizer has migrated or has been improperly spread to the west side of the site. The last thing to note is the sharp drop off of SC from 9 to 12 inches. While SC does significantly decrease in this area, specifications call for this depth to remain untreated. Reasons for SC found at this depth may be a

result of imprecise mixing depth on the mixing machines or leaching of stabilizer from the layers above this depth.

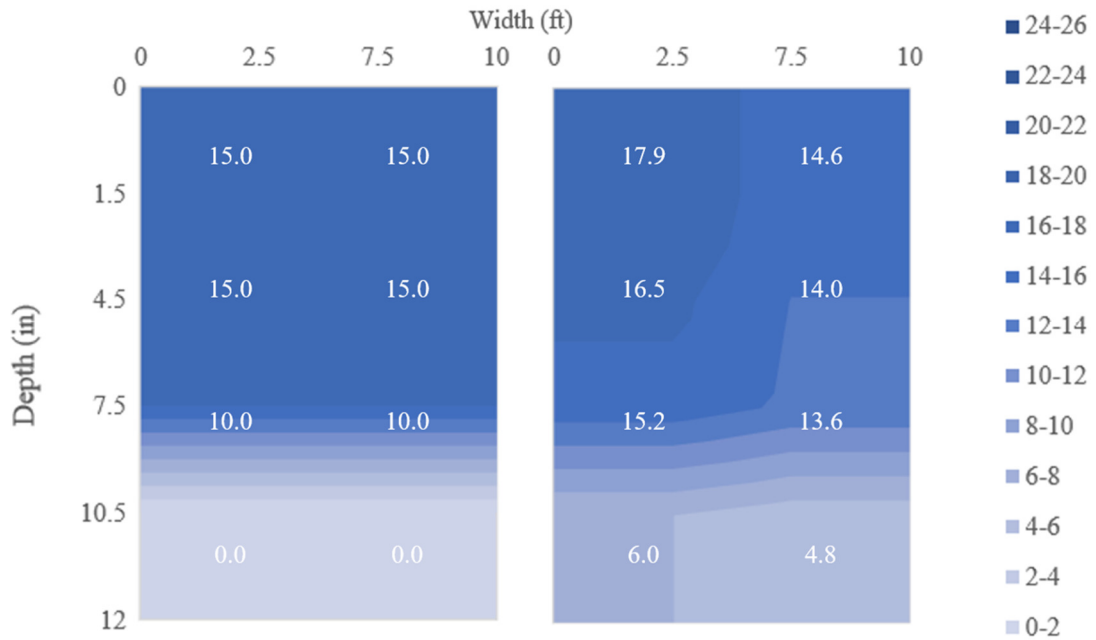


Figure 39: Idealized (Left) and Corrected (Right) Depth Heterogeneity for Site 1

4.3.4.2 Site 2

The idealized depth distribution of *SC* and corrected ex situ PHXRF measurements with depth for Site 2 are illustrated in Figure 40. *SC*s also decrease with depth in this site. For depths 0 to 3, 3 to 6, 6 to 9, and 9 to 12 in, the corrected *SC*s on average are measured as 15.0%, 12.2%, 10.6% and 2.8%, respectively. These measured *SC*s are relatively low compared to the design fly ash *SC* of 16%. Similarly to Site 1, the stabilizer is unproportionally distributed to the west side of the site. Also similarly to Site 1, *SC* reduces significantly in the 9 to 12 inch layer. It

still, however, contains traces of SC, which conflicts with design specifications.

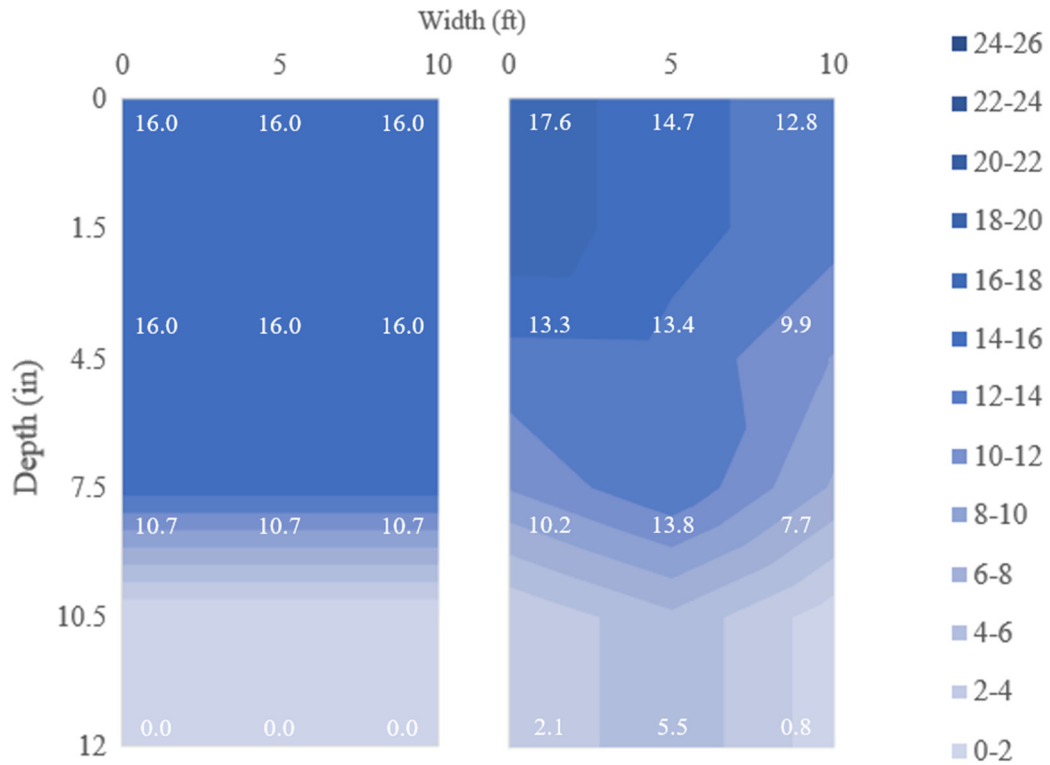


Figure 40: Idealized (Left) and Corrected (Right) Depth Heterogeneity for Site 2

4.3.4.3 Site 3

Site 3 follows the same trends as Sites 1 and 2; SCs decrease with depth for the layers that were able to be sampled. The idealized depth distribution of SC and corrected ex situ PHXRF measurements with depth for Site 3 are illustrated in Figure 41. For depths 0 to 3 and 3 to 6 inches, the corrected SCs on average are measured as 11.3% and 10.4%, respectively. These SCs are relatively close to the design portland cement content of 10%. Measurements below 6 inches were unable to be obtained

due to the stabilized subgrade setting up too quickly. Consequentially, the drop off of *SC* in the 9 to 12 inch layer cannot be analyzed.

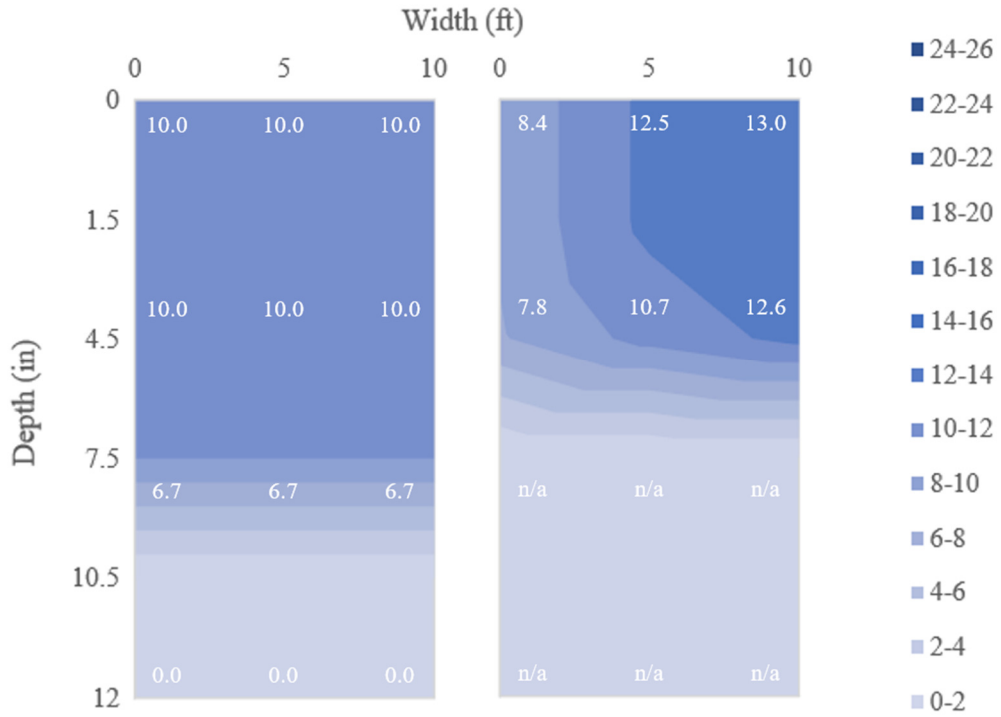


Figure 41: Idealized (Left) and Corrected (Right) Depth Heterogeneity for Site 3

CHAPTER 5

CONCLUSIONS AND RECOMMENDATIONS

5.1 Conclusions

The purpose of this research was to validate PHXRF on stabilized subgrade projects for construction quality control and geotechnical forensic investigations. This was achieved through two comprehensive rounds of experiments: laboratory testing and field testing. Laboratory testing sought to assess the effects of scan duration, scan technique, sample particle size, and sample type on the precision and accuracy of the *SC* measurements of the PHXRF devices. Field testing sought to assess the in situ and ex situ accuracy of the *SC* measurements from the PHXRF devices as well as assess relative spatial and depth *SC* homogeneity of the tested sites. This study ultimately aimed to answer the following questions:

1. What preparation technique yields the most accurate PHXRF *SC* measurements?
Is this preparation technique feasible in the field?
2. What PHXRF device and analysis method should be used to achieve the most accurate PHXRF *SC* measurements?
3. What is the precision and accuracy of in situ and ex situ PHXRF *SC* measurements? Is PHXRF spectrometry a viable option for measuring *SC* in stabilized subgrade soils?
4. Is PHXRF spectrometry a viable option for assessing spatial and depth homogeneity in the field?

The main findings of the research are detailed in Chapter 4. This chapter will synthesize the findings to answer the questions stated above.

1. What preparation technique yields the most accurate PHXRF *SC* measurements? Is this preparation technique feasible in the field?
 - a. Longer scan durations neither improve nor hinder PHXRF precision and accuracy and are therefore considered negligible. For the sake of efficiency, all PHXRF measurements should be limited to 60 seconds.
 - b. Strong correlations are present between smaller particle size samples and improved PHXRF accuracy, but not precision. The samples with particle sizes passing the No. 200 sieve have the smallest variability in discrete measurements relative to the true *SC* of the soil, whereas the passing No. 4 sieve samples have the largest. This is likely due to the reduction of elemental concentrations by milling. Milling samples passed the No. 200 sieve, however, is not very practical in the field. Significant benefits in terms of PHXRF accuracy are observed when particle sizes are reduced from passing No. 4 to passing No. 40, yet the benefits are less significant when particle sizes are reduced further. Field preparation should be limited to milling samples passed a No. 40 sieve.
 - c. The relationship between sample type and the precision and accuracy of the PHXRF devices is inconclusive due to conflicting results between OHC and SGB samples. It should be noted that the preparation of pressed pellets is a laborious endeavor. It takes approximately 15 minutes to produce one pressed pellet sample, whereas it only takes approximately

one minute to produce a powder sample. In some cases, such as field applications where hundreds of samples may need to be processed, it may be reasonable to forgo the increase in measurement accuracy from pressed pellets for practicality purposes.

2. What PHXRF device and analysis method should be used to achieve the most accurate PHXRF *SC* measurements?

- a. Either a standard scanning technique, where a sample is scanned at the same location three times, or a quartering scanning technique, where a sample is rotated 90° after each scan, may be appropriate for PHXRF *SC* measurements. Quartering techniques, however, provide a unique opportunity to assess sample homogeneity if the PHXRF in use has a small X-ray beam footprint.
- b. The S1 Titan PHXRF had far more accurate measurements for the OHC samples, whereas the Niton XL3t had far more accurate measurements for the SGB samples. This may be more of a testament to the factory soil calibrations on the respective devices as opposed to their limitations. In an unknown soil situation, the Niton XL3t is the more appropriate device to use because its deviations relative to the true *SC* are on average less than those of the S1 Titan.

3. What is the precision and accuracy of in situ and ex situ PHXRF *SC* measurements? Is PHXRF spectrometry a viable option for measuring *SC* in stabilized subgrade soils?

- a. The PHXRF device performed poorly in situ. The average STDEV for these measurements is upwards of 2.1%, the RMSD upwards of 24.0%, and no linear relationship between in situ measurements and true *SC*s is observed in the data. These inaccuracies are not surprising though because the literature heavily stresses the importance of sample preparation. Possible causes for in situ inaccuracies could be a number of things like excessive surface roughness, the presence of elemental concentrations, the presence of oxygen, wind blowing material into the scan window, and the presence of moisture. It is for many of these reasons that in situ measurements are deemed inadequate when determining *SC* in subgrade soils.
 - b. The PHXRF device performed well ex situ. The STDEV was steady around 0.449% and the RMSD around 9.818%, which is about half of those observed in the in situ measurements. While these errors are far outside of limitations, they are consistent and remarkably linear. The linear relationship between ex situ measurements and true *SC*s has an R^2 value of 0.925. Therefore, ex situ measurements can be mathematically corrected using the equation of the regression line between ex situ measurements and true *SC*s. Consequentially, corrected ex situ PHXRF *SC* measurements may be a viable option for determining *SC* in stabilized subgrade soils.
4. Is PHXRF spectrometry a viable option for assessing spatial and depth homogeneity in the field?

- a. The PHXRF device proved to be a useful tool when assessing spatial distribution of *SC* throughout three tested sites. The average *SC*s measured in the design volume of the sites are often within $\pm 1\%$ of the design *SC*, which is encouraging. Spatial variability is found to be an issue on all sites. PHXRF is a very helpful and convenient way of gathering the data needed to assess the spatial heterogeneity of stabilized subgrade sites.
- b. The PHXRF device proved to be a useful tool when assessing depth distribution of *SC* for many of the same reasons as stated for the spatial distribution assessment. The PHXRF measurements detect a decrease in *SC* throughout the design depth of all three sites. Additionally, the device measures notable amounts of chemical stabilizer below the design depth, which conflicts with specifications. These measurements are easily used to populate a contour chart to illustrate depth heterogeneity throughout stabilized subgrade sites.

Cultivating this technology aligns directly with the Southern Plains Transportation Center's (SPTC) mission to develop comprehensive, cost-effective, and imminently implementable solutions to critical infrastructure-related issues facing the transportation systems of the region and the nation. Creating an accurate, portable, and efficient method for determining *SC* will enable inspectors to enact improved quality control measures during constructions, leading to more reliable and safer roadways. Additionally, this technology will save time and provide more complete data during forensic geotechnical investigations, leading to cost savings and a deeper understanding

of stabilization issues. It is the authors hope that this technology will lead to higher quality roadways at levels previously unobtainable.

5.2 Recommendations for Future Research

Before the push for policy changes is made to include PHXRF spectrometry as part of the quality control protocols for subgrade stabilization in the southern plains states, more field testing will need to be completed to further verify the accuracy and feasibility of implementing this technology. It is recommended that two to seven more subgrade stabilization sites be measured. Additionally, it may be beneficial to retain stabilized subgrade samples from around the region to build an application specific calibration on the PHXRF devices. This will take thousands of samples to create a comprehensive reference library for the device to compare a discrete measurement to. The only way to build such an elaborate library is to continuously add known samples over a period of time.

An additional research recommendation includes conducting further studies on pressed pellet versus powder samples to determine conclusively which sample type is more conducive for PHXRF *SC* measurements. Also, it may be beneficial to look into why OHC and SGB samples so often yielded conflicting results. Perhaps PHXRF *SC* measurements may be affected by the mineralogy of the samples.

Furthermore, it may be beneficial to examine leaching in stabilized soils. Laboratory tests may be able to determine how fast and how much stabilizer leaches from stabilized soils. PHXRF spectrometry can then be used to determine how much stabilizer to add back into the soil for it to achieve its design strength.

CHAPTER 6

SCHEDULE

Date	Location	Activity
October 2013 - May 2014	The University of Oklahoma	Literature Review Learn science behind XRF Spectrometry Review XRF sample preparation methods Learn limitations of XRF spectrometry Survey current subgrade stabilization methods Review soil analysis with XRF spectrometry
May - July 2014	The University of Oklahoma and ODOT Materials Laboratory	XRF Sample Preparation Complete mix design of soil/stabilizer samples Mix samples to various stabilizer contents Mill samples to specified fineness Create pressed pellet and powder samples
July 2014	The University of Oklahoma	Laboratory Testing with PHXRF Spectrometer Take CaO measurements with Bruker S1 Titan
July - December 2014	The University of Oklahoma	Analyze PHXRF Data Analyze precision and accuracy of Bruker S1 Titan Determine if scan intervals affect accuracy Determine if sample particle size affects accuracy
January 2015	The University of Oklahoma	Laboratory Testing with PHXRF Spectrometer Take CaO measurements with Niton XL3t GOLDD+
January - May 2015	The University of Oklahoma	Analyze PHXRF Data Analyze precision and accuracy of Niton XL3t GOLDD+ Determine if sample particle size affects accuracy Determine if scan technique affect accuracy Compare accuracy between the two XRF devices
May - September 2015	Various Construction Sites	Field Testing with PHXRF Spectrometer Take CaO measurements with Niton XL3t GOLDD+ Collect samples to bring back to the laboratory
September - December 2015	The University of Oklahoma	Analyze PHXRF Data Compare field accuracy to laboratory accuracy Identify trends in the data Identify possible sources of error Develop field methodology Make recommendations regarding application
December 2015 - April 2016	The University of Oklahoma	Write Thesis
April 2016	The University of Oklahoma	Defend Thesis

CHAPTER 7

REFERENCES

- Abdelbagi, M., Eltayeb, M., Rahman, S., and M. Elboraie. "Source Identification of Airborne Elements in Industrial Area by XRF Technique." *Indian Journal of Science and Technology*, Vol. 4 No. 7 (2011): 824-827. Web. 4 Dec. 2015.
- American Society of Civil Engineers. "Code of Ethics." ASCE.org. ASCE, 23 Jul. 2006. Web. 5 Mar. 2015.
- Arkansas State Highway and Transportation Department. *Arkansas 2014 Standard Specification for Highway Construction*. Little Rock: Arkansas State Highway and Transportation Department, 2014. Web. 20 Oct. 2015.
- Arora, S. and A. Aydilek. "Class F Fly Ash Amended Soils as Highway Base Materials." *Journal of Materials in Civil Engineering*, Vol. 17 No. 6 (2005): 640-649. Web. 24 Nov. 2015.
- Arzhantsev, S., Li, X., and J. Kauffman. "Rapid Limit Tests for Metal Impurities in Pharmaceutical Materials by X-ray Fluorescence Spectroscopy Using Wavelet Transform Filtering." *Analytical Chemistry*, Vol. 83 (2011): 1061-1068. Web. 4 Dec. 2015.
- ASTM D3155-11: Standard Test Method for Lime Content of Uncured Soil-Lime Mixtures, *Annual Book of ASTM Standards*, ASTM International, West Conshohocken, PA, 2011.
- ASTM D2216-10: Standard Test Method for Laboratory Determination of Water (Moisture) Content of Soil and Rock by Mass, *Annual Book of ASTM Standards*, ASTM International, West Conshohocken, PA, 2010.
- ASTM D422-63(2007)e2: Standard Test Method for Particle-Size Analysis of Soils, *Annual Book of ASTM Standards*, ASTM International, West Conshohocken, PA, 2007.
- Athanasopoulou, A. "Addition of Lime and Fly Ash to Improve Highway Subgrade Soils." *Journal of Materials in Civil Engineering*, Vol. 26 No. 4 (2014): 773-775. Web. 24 Nov. 2015.
- Aykut, S., Edil, T., Bin-Shafique, M., Acosta, H., and C. Benson. "Soft Subgrades' Stabilization by Using Various Fly Ashes." *Resources, Conservation and Recycling*, Vol. 46 (2006): 365-376. Web. 24 Nov. 2015.

- Barkla, C. and A. Sadler. "The Absorption of X-rays." *Nature*, Vol. 80 No. 2054 (1909): 37. Web. 5 Dec. 2015.
- Bell, F. "Lime Stabilization of Clay Soils." *Bulletin of the International Association of Engineering Geology*, Vol. 39 No. 1 (1989): 67-74. Web. 24 Nov. 2015.
- Binstock, D., Gutknecht, W., and A. McWilliams. "Lead in Soil by Field-Portable X-ray Fluorescence Spectrometry - An Examination of Paired In Situ and Laboratory ICP-AES Results." *REMEDIATION*, Summer (2008): 55-61. Web. 4 Dec. 2015.
- Bruker. "How Does X-Ray Fluorescence (XRF) Work?" *S2 Ranger Brochure*. Bruker, 2013. Web. 29 Mar. 2016.
- Cerato, A. and G. Miller. "Determination of Soil Stabilizer Content Using X-ray Fluorescence." *Geotechnical Testing Journal*, Vol. 36, No. 5 (2013): 781-785. PDF.
- Elliot, R., Dennis, N., and Y. Qiu. "Permanent Deformation of Subgrade Soils." Mack-Blackwell Transportation Center FR 1069 (1998). Web. 24 Nov. 2015.
- Forster, N. and P. Grave. "Non-Destructive PXRF Analysis of Museum-Curated Obsidian from the Near East." *Journal of Archaeological Science*, Vol. 39: 728-736. Web. 4 Dec. 2015.
- Frahm, E. "Validity of "Off-the-Shelf" Handheld Portable XRF for Sourcing Near Eastern Obsidian Chip Debris." *Journal of Archaeological Science*, Vol. 40 (2013): 1080-1092. 4. Dec. 2015.
- Fredlund, D. "The Prediction and Performance of Structures on Expansive Soils." *Proceedings, Predication, and Performance in Geotechnical Engineering*. Calgary, AB. 17-19 Jun. 1987. Web. 24 Nov. 2015.
- Gatz, T. "Oklahoma Transportation Research Day." Oklahoma Department of Transportation and Southern Plains Transportation Center. Moore Norman Technology Center, Oklahoma City, OK. 20 Oct. 2015. Address.
- Holland, J. and C. Griffin. "Cement and Lime Stabilization of Melbourne Pavement Subgrade Soils." *3rd Australia-New Zealand Conference of Geomechanics*, Vol. 1 (1980): 1191-1195. Web. 24 Nov. 2015.
- Houston, S. "Pavement Problems Caused by Collapsible Subgrades." *Journal of Transportation Engineering*, Vol. 114 No. 6 (1988): 673-683. Web. 25 Nov. 2015.
- Houston, S., Houston, W., and C. Lawrence. "Collapsible Soil Engineering in Highway Infrastructure Development." *Journal of Transportation Engineering*, Vol. 128 No. 3 (2002): 295-300. Web. 25 Nov. 2015.

Howayek, A., Huang, P., Bisnett, R., and M. Santagata. "Identification and Behavior of Collapsible Soils." Joint Transportation Research Program Technical Report 2011/12 (2011). Web. 25 Nov. 2015.

Huang, Y. "Pavement Analysis and Design 1st Edition." Englewood Cliffs: Prentice Hall, 1993. Web. 24 Nov. 2015.

Hürkamp, K., Raab, T., and J. Völkel. "Two and Three-Dimensional Quantification of Lead Contamination in Alluvial Soils of a Historic Mining Area Using Field Portable X-ray Fluorescence (FPXRF) Analysis." *Geomorphology*, No. 110 (2009): 28-36. Web. 4 Dec. 2015.

Imanishi, Y., Bando, A., Komatani, S., Wada, S., and K. Tsuji. "Experimental Parameters for XRF Analysis of Soils." *International Centre for Diffraction Data* (2010): 248-255. Web. 26 Jan. 2015.

Insley, H. and R. Ewell. "Thermal Behavior of the Kaolin Minerals." *Journal of Research of the National Bureau of Standards*, Vol. 14 (1935): 615-627. Web. 4 Dec. 2015.

Kim, N., Kim, J., Ahn, K., and B. Lee. "Use of Field-Portable X-ray Fluorescence (FPXRF) Analyzer to Measure Airborne Lead Levels in Korean Workplaces." *Journal of Occupational Health*, Vol. 49 (2007): 493-498. Web. 4 Dec. 2015.

Kolias, S., Kasselouri-Rigopoulou, V., and A. Karahalios. "Stabilisation of Clayey Soils with High Calcium Fly Ash and Cement." *Cement & Concrete Composites*, Vol. 27 (2005): 301-313. Web. 24 Nov. 2015.

Krohn, J., and J. Slosson. "Assessment of Expansive Soils in the United States." *Conference Proceedings. 4th International Conference on Expansive Soil* (1980): 596-608. Web. 24 Nov. 2015.

Krusberski, N. "Exploring Potential Errors in XRF Analysis." Analytical Challenges in Metallurgy. The Southern African Institute of Mining and Metallurgy. Johannesburg: SAIMM, 2006. 1-8. Web. 26 Jan. 2015.

Kulikov, E., Latham, K., and M. Adams. "Classification and Discrimination of Some Cosmetic Face Powders using XRF Spectrometry with Chemometric Data Analysis." *X-ray Spectrometry*, Vol. 41 (2012): 410-415. Web. 4 Dec. 2015.

Lawton, E., Fragaszy, R., and M. Hetherington. "Review of Wetting-Induced Collapse in Compacted Soil." *Journal of Geotechnical Engineering*, Vol. 118 No. 9 (1992): 1376-1394. Web. 24 Nov. 2015.

- Li, L., Edil, T. and C. Benson. "Properties of Pavement Geomaterials Stabilized with Fly Ash." *2009 World of Coal Ash Conference*, University of Kentucky Center for Applied Energy Research, Lexington, KY, 2009. Web. 24 Nov. 2015.
- Lin, B., Cerato, A., Madden, A., and M. Madden. "Effect of Fly Ash on the Behavior of Expansive Soils: Microscopic Analysis." *Environmental & Engineering Geoscience*, Vol. 19 No. 1 (2013): 85-94. Web. 24 Nov. 2015.
- Louisiana Department of Transportation and Development. *Louisiana Standard Specifications for Roads and Bridges*. Baton Rouge: Louisiana Department of Transportation and Development, 2006. Web. 20 Oct. 2015.
- Majidzadeh, K., Bayomy, F., and S. Khedr. "Rutting Evaluation of Subgrade Soils in Ohio." *Transportation Research Record* 671 (1978): np. Web. 24 Nov. 2015.
- Marguí, E., Van Meel, K., Van Grieken, R., Buendía, A., Fontàs, C., Hidalgo, M., and I. Queralt. "Method for the Determination of Pd-Catalyst Residues in Active Pharmaceutical Ingredients by Means of High-Energy Polarized-Beam Energy Dispersive X-ray Fluorescence." *Analytical Chemistry*, Vol. 81 (2009): 1404-1410. Web. 4 Dec. 2015.
- Markowicz, A. "An Overview of Quantification Methods in Energy-Dispersive X-ray Fluorescence Analysis." *Pramana Journal of Physics*, Vol. 76 No. 2 (2011): 321-329. Web. 26 Jan. 2015.
- Maruyama, Y., Ogawa, K., Okada, T., and M. Kato. "Laboratory Experiments of Particle Size Effect in X-ray Fluorescence and Implications to Remote X-ray Spectrometry of Lunar Regolith Surface." *Earth Planets Space*, Vol. 60 (2008): 293-297. Web. 26 Jan. 2015.
- Millhauser, J., Rodríguez-Alegría, E., and M. Glascock. "Testing the Accuracy of Portable X-ray Fluorescence to Study Aztec and Colonial Obsidian Supply at Xaltocan, Mexico." *Journal of Archaeological Science*, Vol. 38 (2011): 3141-3152. Web. 4 Dec. 2015.
- Mishra, A., Dhawan, S., and R Sudhakar. "Analysis of Swelling and Shrinkage Behavior of Compacted Clays." *Geotechnical and Geological Engineering*, Vol. 28 (2008): 289-298. Web. 25 Nov. 2015.
- Moradi, M., Zenouzi, S., Ahmadi, K., and A. Aghakhani. "Graphene Oxide-Based Solid Phase Extraction of Vitamin B₁₂ from Pharmaceutical Formulations and its Determination by X-ray Fluorescence." *X-ray Spectrometry*, Vol. 44 (2015): 16-23. Web. 4 Dec. 2015.
- Moseley, H. "High Frequency Spectra of Elements." *The Philosophers Magazine*, Vol. 26 (1913): 1024-1034. Web. 6 Dec. 2015.

Moseley, H. "High Frequency Spectra of Elements." *The Philosophers Magazine*, Vol. 27 (1914): 703-713. Web. 6 Dec. 2015.

National Lime Association. "Lime-Treated Soil Construction Manual: Lime Stabilization & Lime Modification." Arlington: National Lime Association, Bulletin 326, 2004. Web. 24 Nov. 2015.

New Mexico Department of Transportation. *Standard Specifications for Highway and Bridge Construction 2014 Edition*. Santa Fe: New Mexico Department of Transportation, 2014. Web. 20 Oct. 2015.

Oklahoma Department of Transportation. *2009 Standard Specifications Book*. Oklahoma City: Oklahoma Department of Transportation, 2009. Web. 20 Oct. 2015.

Ortiz, R., Mariotti, K., Schwab, N., Sabin, G., Rocha, W., Castro, E., Limberger, R., Mayorga, P., Bueno, M., and W. Romão. "Fingerprinting of Sildenafil Citrate and Tadalafil Tablets in Pharmaceutical Formulations via X-ray Fluorescence (XRF) Spectrometry." *Journal of Pharmaceutical and Biomedical Analysis*, Vol. 58 (2012): 7-11. Web. 4 Dec. 2015.

Palmer, P., Jacobs, R., Baker, P., Ferguson, K., and S. Webber. "Use of Field-Portable XRF Analyzers for Rapid Screening of Toxic Elements in FDA-Regulated Products." *Journal of Agriculture and Food Chemistry*, Vol. 57 No. 7 (2009): 2605-2613. Web. 4 Dec. 2015.

Parsons, C., Grabulosa, E., Pili, E., Floor, G., Roman-Ross, G., and L. Charlet. "Quantification of Trace Arsenic in Soils by Field-Portable X-ray Fluorescence Spectrometry: Considerations for Sample Preparation and Measurement Conditions." *Journal of Hazardous Materials*, Vol. 262 (2013): 1213-1222. Web. 4 Dec. 2015.

Parsons, R., Keebone, E., and J. Milburn. "Use of Cement Kiln Dust for Subgrade Stabilization." Kansas Department of Transportation Final Report KS-04-3 (2004). Web. 25 Nov. 2015.

Patterson, M. "Oklahoma Transportation Research Day." Oklahoma Department of Transportation and Southern Plains Transportation Center. Moore Norman Technology Center, Oklahoma City, OK. 20 Oct. 2015. Keynote Speaker.

Ramsey, Rick. Personal Interview. 12 Feb. 2014.

Salahudeen, A., Eberemu, A., and K. Osinubi. "Assessment of Cement Kiln Dust-Treated Expansive Soil for the Construction of Flexible Pavements." *Geotechnical and Geological Engineering*, Vol. 32 No. 4 (2014): 923-931. Web. 25 Nov. 2015.

Shackley, S. *X-ray Fluorescence Spectrometry (XRF) in Geoarchaeology*. New York: Springer Science+Business Media, LLC, 2011. Web. 3 Dec. 2015.

Singh, S. *Critical Reasons for Crashes Investigated in the National Motor Vehicle Crash Causation Survey*. Washington: GPO, 2015. Web. 5 Mar. 2015.

Solanki, P., Khoury, N., and M. Zaman. "Engineering Properties of Stabilized Subgrade Soil for Implementation of the AASHTO 2002 Pavement Design Guide." Final Report - FHWA-OK-08-10 ODOT SPR Item Number 2185 (2009). 4 Dec. 2015.

Sun, Z., Quan, Y., and Y. Sun. "Elemental Analysis of White Electrical Tapes by Wavelength Dispersive X-ray Fluorescence Spectrometry." *Forensic Science International*, Vol. 232 (2013): 169-172. Web. 4 Dec. 2015.

Texas Department of Transportation. *Standard Specifications for Construction and Maintenance of Highways, Streets, and Bridges*. Austin: Texas Department of Transportation, 2014. Web. 20 Oct. 2015.

United States Department of Transportation. Federal Highway Administration. Office of Highway Policy Information. *Our Nation's Highways 2000*. Washington: GPO, 2000. Web. 5 Mar. 2015.

United States Department of Transportation. Federal Highway Administration. Office of Highway Policy Information. *Our Nation's Highways 2011*. Washington: GPO, 2011. Web. 5 Mar. 2015.

Zawisza, B. and R. Sitko. "Determination of Trace Elements in Suspension and Filtrates of Drinking and Surface Water by Wavelength-Dispersive X-ray Fluorescence Spectrometry." *Analytical and Bioanalytical Chemistry*, Vol. 384 (2006): 1600-1604. Web. 4 Dec. 2015.